



Fine-scale fluctuations of PM_1 , $PM_{2.5}$, PM_{10} and SO_2 concentrations caused by a prolonged volcanic eruption (Fagradalsfjall 2021, Iceland)

Rachel C. W. Whitty¹, Evgenia Ilyinskaya¹, Melissa A. Pfeffer², Ragnar H. Thrastarson², Þorsteinn Johannsson³, Sara Barsotti², Tjarda J. Roberts^{4, 5}, Guðni M. Gilbert^{2, 9}, Tryggvi Hjörvar², Anja Schmidt^{6, 7, 8}, Daniela Fecht¹⁰, Grétar G. Sæmundsson¹¹

¹COMET, Institute of Geophysics and Tectonics, School of Earth and Environment, University of Leeds, Leeds, LS2 9JT, United Kingdom

10 ²Icelandic Meteorological Office, 150 Reykjavík, Iceland

³The Environment Agency of Iceland, 108 Reykjavík, Iceland

⁴CNRS UMR7328, Laboratoire de Physique et de Chimie de l'Environnement et de l'Espace, Université d'Orleans, Orleans, 45071, France

15 ⁵LMD/IPSL, ENS, Université PSL, École Polytechnique, Institut Polytechnique de Paris, Sorbonne Université, CNRS, F-75005 Paris, France

⁶Yusuf Hamed Department of Chemistry, University of Cambridge, Cambridge, CB2 1EW, United Kingdom

⁷Institute of Atmospheric Physics (IPA), German Aerospace Centre (DLR), 82234 Oberpfaffenhofen, Germany

⁸Meteorological Institute, Ludwig Maximilian University of Munich, 80333 Munich, Germany

⁹Nox Medical, 150 Reykjavík, Iceland

20 ¹⁰MRC Centre for Environment and Health, School of Public Health, Imperial College London, London, W12 0BZ, United Kingdom

¹¹Department of Research and Analysis, Icelandic Tourist Board, 101 Reykjavík, Iceland

Correspondence to: Evgenia Ilyinskaya (e.ilyinskaya@leedss.ac.uk)

25

Abstract.

The 2021 Fagradalsfjall fissure eruption was the first of multiple ongoing eruptions in the most densely populated part of Iceland (70% of population within 50 km). It was monitored by an exceptionally dense reference-grade air quality network (14 stations within 40 km), and the first time that a reference-grade timeseries of PM_1 was collected during an eruption. We used these measurements to investigate fine-scale dispersion patterns of volcanic pollutants (SO_2 , PM_1 , $PM_{2.5}$, PM_{10}) in populated areas.

30



Despite its small size the eruption caused a statistically-significant increase in average and peak **PM** and SO₂ concentrations in at least 300 km distance. Peak daily-means of PM₁ peak rose to 18-20 µg/m³ from 5-6 µg/m³, and **proportion** of PM₁ increased relative to coarser PM fractions (21-24% of PM₁₀ compared to 14% background). **Eruption** increased PM₁₀ and PM_{2.5} by ~50% in populated areas with low background concentrations, but its impact was not measurable in areas with high background sources. This suggests that ash-poor eruptions are one of, or the most, important source of PM₁ in Iceland, and potentially in other areas exposed to volcanic emissions.

There were significant fine-scale temporal (≤1 hour) and spatial (<1 km) fluctuations in volcanic pollutant concentrations. In Reykjavík, two stations located **<1 km of each** other recorded peak hourly-mean concentrations of 480 and 250 µg/m³ SO₂, and 5 and 0 exceedance events, respectively, within a ~12-hour plume advection event. This has implications for population exposures estimates.

1 Introduction

Globally, over a billion people are estimated to live within 100 km of an active volcano (Freire et al., 2019), a distance within which they might be exposed to volcanic air pollution (Stewart et al., 2021), and the number of potentially exposed people is growing because of building expansion into previously uninhabited areas near volcanoes. Basaltic fissure eruptions happen frequently near populated areas, for example at Kīlauea volcano on Hawaii (tens of episodes since 1983), Cumbre Vieja on La Palma 2021 and currently on Reykjanes, Iceland (from 2021 and ongoing at the time of writing). Even small, ash-poor fissure eruptions can cause severe air pollution episodes when they happen at the urban interface (Whitty et al., 2020).

Throughout this work, we will refer to ‘volcanic emissions’, and unless otherwise stated, our intended meaning is SO₂ gas and **PM** (primary and secondary), collectively. Prior to this study, the best observed and studied impacts of volcanic emissions on air quality came from Kīlauea in Hawaii (in particular the 2018 large fissure eruption), and **Holuhraun** large fissure eruption 2014-2015 in Iceland. Both of these volcanic sources degraded air quality at distances of hundreds of kilometres during times of activity (Crawford et al., 2021; Gíslason et al., 2015; Ilyinskaya et al., 2017; Schmidt et al., 2015; Whitty et al., 2020). A public health investigation of the Holuhraun eruption showed that it was associated with an increase in register-measured health care utilisation for respiratory disease in Iceland’s capital area 250 km from **source** (Carlsen et al., 2021a, b). The studies **of** Kīlauea and Holuhraun 2014-2015 eruptions were based on observations from relatively few and distal air quality stations; the closest **reference-grade** station to Holuhraun was at ~90 km distance, and ~40 km distance at Kīlauea. When the reference-grade air quality network on Hawaii was augmented by 16 **low-cost** SO₂ and PM_{2.5} sensors during a two-week campaign in 2018 it was shown that estimates of population exposure to volcanic air pollution can change significantly with a denser sensor network (Crawford et al., 2021). Studies of volcanic plume chemistry in Holuhraun and Kīlauea eruptions have hypothesized that there may be significant fine-scale fluctuations in concentrations and dispersion



patterns of volcanic gas and PM, potentially very close to the eruption site (Ilyinskaya et al., 2017, 2021), but this has not yet been observed in the field.

65 Fagradalsfjall 2021 was a small fissure eruption that happened in the most densely populated part of Iceland (>260,000 people or ~70% of the country's population lived within 40 km distance from the eruption site). The studies on Holuhraun 2014-2018 and Kilauea 2018 eruptions made important discoveries about distal air quality impacts of large fissure eruptions (erupted volume km^3), which took place in relatively sparsely populated areas. Small eruptions (erupted volume from <0.1 up to 1 km^3) are very important to investigate with regards to air pollution because they account for ~80% of eruptions worldwide (Siebert et al., 2015), and their impact on populated areas is likely to increase as the global population grows. Fagradalsfjall 2021 presented a unique opportunity to advance our understanding of the intensity and dispersion patterns of volcanic air pollution in downwind populated areas. It was monitored by the densest reference-grade air quality monitoring network of any volcano in the world (to our knowledge) with 27 stations across Iceland, thereof 14 stations within 40 km distance from the eruption site. Some of these stations were located within 1 km from one another. This allowed our investigation into very fine-scale changes in spatial and temporal air quality impacts with respect to sulphur dioxide (SO_2), and different particulate matter size fractions (PM_{10} , $\text{PM}_{2.5}$, PM_{10}), which are the volcanic air pollutants that are likely to be elevated, both at source and at significant distances downwind (Stewart et al., 2021). This is also the first study reporting on a reference-grade timeseries of PM_{10} during a volcanic eruption. PM_{10} is known to be the dominant size fraction in volcanic emissions when measured directly at the volcanic source, but it has never been measured in downwind populated areas impacted by a volcanic eruption. Evidence-based air quality thresholds have been defined for SO_2 , $\text{PM}_{2.5}$ and PM_{10} but not yet for PM_{10} , largely due to the paucity of reference-grade data on concentrations and dispersion (World Health Organization, 2021). PM_{10} is only recently being introduced in operational air quality monitoring worldwide (from 2020 in Iceland) and evidence-based guidelines for its levels are not yet established. Available studies unequivocally demonstrate a correlation between increased concentrations of PM_{10} and negative health outcomes (Chen et al., 2017; Wang et al., 2011; Yang et al., 2018) and high-quality datasets on levels and variability of PM_{10} are therefore important steps towards establishing air quality guidelines.

1.1 Fagradalsfjall 2021 eruption description

Fagradalsfjall 2021 (19 March - 19 September 2021) was the first eruption to happen in the most densely populated area of Iceland in ~800 years, and is considered to have been the beginning of a prolonged eruptive period on the Reykjanes peninsula, locally known as Reykjanes Fires. At the time of writing, there have been 9 further eruptions on Reykjanes peninsula, thereof two in the Fagradalsfjall volcanic system (August 2022 and July 2023), and seven in the adjacent Reykjanes-Lavatsengi system (December 2023 – November 2024). Magma accumulation currently continues and based on the eruption history of the Reykjanes peninsula, eruptive episodes activity may occur repeatedly for decades or centuries. Fagradalsfjall 2021 was a small eruption (total ~0.3 to 0.9 Mt SO_2 , 4.82 km^2 lava (Barsotti et al., 2023; Pfeffer et al., 2024)) but due to its location and population growth it may have exposed more people to volcanic air pollution than any previous



eruption in the country (Fig. 1). The eruption behaviour was very dynamic, and the number of active craters and the eruptive style changed several times during its duration; for further details see (Barsotti et al., 2023). The eruption site was at 9 km distance from the closest town of Grindavík; and over 70% of Iceland’s total population (263,000 out of 369,000 people) lived within 50 km distance, including the capital area of Reykjavík. The easily accessible site was also visited by ~300,000 people for sightseeing during its course.

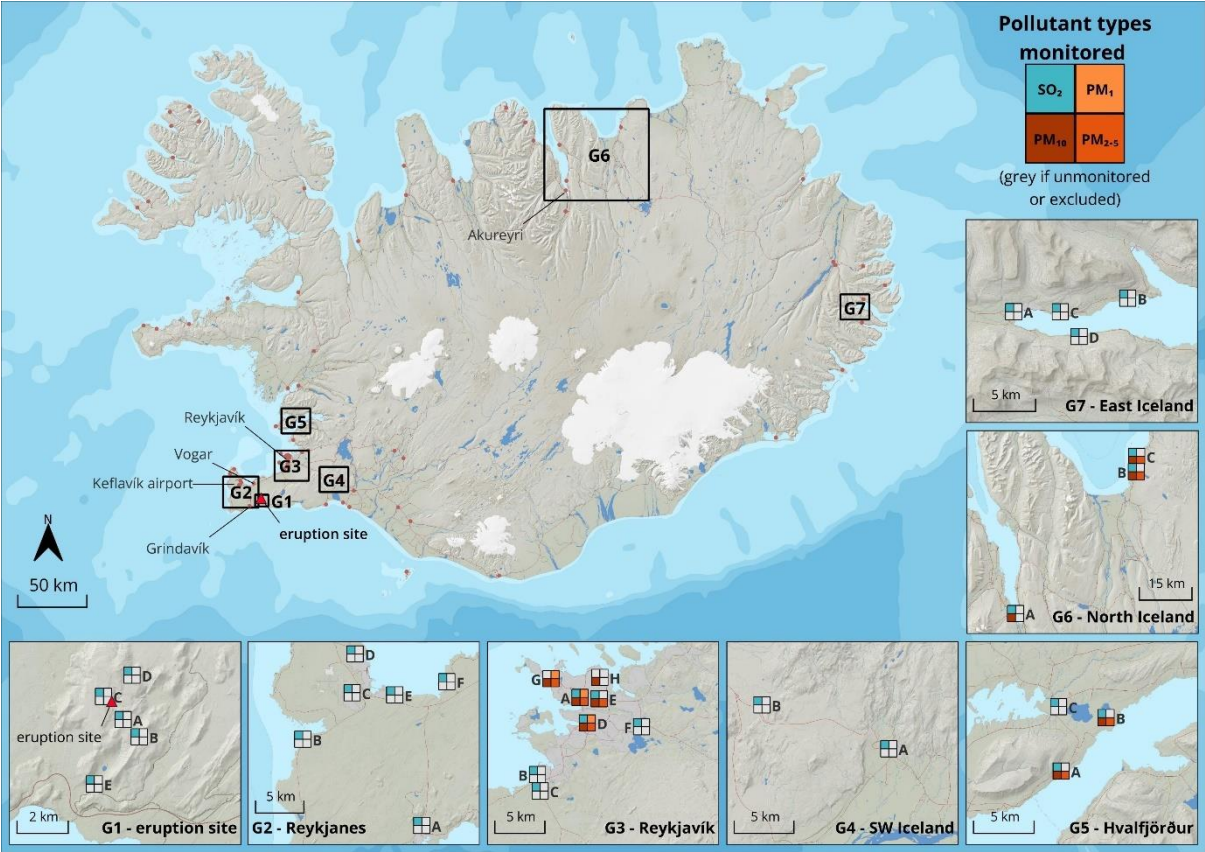


Figure 1: Map of Iceland showing the eruption site and air quality monitoring stations. The stations were organised in 7 geographic clusters (each shown on the enlarged inserts). G1 - Eruption site (0-4 km distance from the volcanic vent). G2 Reykjanes peninsula (9-20 km distance). G3 - Reykjavík capital area (25-35 km distance). G4 - Southwest Iceland (45-55 km distance). G5 - Hvalfjörður (50-55 km distance). G6 - North Iceland (A and B ~280 km, C and D ~330 km distance). G7 - East Iceland (~400 km). The map shows the air pollutant species monitored at each station (SO₂, PM₁₀, PM_{2.5}, PM₁). Areas G2-G7 were monitored with reference-grade stations, while G1 had lower-cost eruption response sensors. Source and copyright of basemap and cartographic elements: Icelandic Met Office & Icelandic Institute of Natural History.



110 2 Methods

Measurements were collected by two types of instrument networks: a reference-grade municipal air quality (AQ) network managed by the Environmental Agency of Iceland (EAI, SO₂ and PM in different size fractions); and an eruption-response gas sensor network operated by the Icelandic Meteorological Office (IMO, SO₂ only).

2.1 Reference-grade municipal network

115 The EAI network monitors air quality across Iceland according to national legal mandates and complies with Icelandic Directive (ID) regulations. Most of the monitoring stations are in populated areas and measure a variety of air pollutants. Here, we analysed SO₂ and PM in PM₁, PM_{2.5}, PM₁₀ size fractions, which are the most important volcanic air pollutants with respect to human health in downwind populated areas (Stewart et al., 2021). The detection limits for the majority of the stations in this study were reported to be ~1-3 µg/m³ SO₂ and < 5 µg/m³ PM. Station-specific instrument details, detection
 120 and resolution limits, and operational duration are in Supplementary Table S1. Figure 1 shows the location of the stations and the air pollutants species measured there.

2.2 Eruption site sensors

At the eruption site (0.6-3 km from the active craters), the IMO installed a network of five lower-cost SO₂ sensors between April and July 2021 to monitor air quality in the near-field (specifications and operational length in Table S1). Figure 1
 125 shows the location of those eruption-response SO₂ sensors. Stations A, B and E were in close proximity to the public footpaths, while stations C and D were further afield to the north and northwest of the eruption site. The main purpose of the eruption-response network was to alert visitors when SO₂ levels were high rather than to provide accurate SO₂ concentrations. This was because lower-cost air quality sensors (gas and PM) are known to be significantly less accurate than reference-grade instruments (Crilley et al., 2018; Whitty et al., 2022, 2020). Whitty et al., 2022 assessed the
 130 performance of lower-cost SO₂ sensors specifically in volcanic environments (same or comparable sensor models to the eruption site stations here) and found that they were frequently subject to interferences restricting their capability to monitor SO₂ in low concentrations. The sensor accuracy limits during field deployment of (Whitty et al., 2022) were significantly poorer than the detection limits reported by the manufacturer. The sensors used in this study were not calibrated or co-located with higher-grade instruments during the field deployment, which seriously limits the accuracy of the obtained data.
 135 Due to the low accuracy of the eruption site sensors, especially at lower concentration levels, we analysed the SO₂ data not quantitatively but as yes/no for exceeding the hourly-mean ID air quality threshold of 350 µg/m³.

2.3 Data processing

SO₂ measurements were downloaded from 24 reference-grade stations and 5 eruption site sensors, and PM₁₀, PM_{2.5} and PM₁ were downloaded from 12, 11 and 3 reference-grade stations, respectively. Data from reference-grade stations were quality



checked and, where needed, re-calibrated by the EAI. Where the operational length was sufficiently long, we obtained SO₂ and PM measurements for both the eruption period and non-eruptive background period.

We excluded from the analysis reference-grade stations that had data missing for more than 4 months (>70%) of the eruption period. Further details on exclusion reasons of individual stations are in Table S1. This criteria excluded both PM₁₀ and PM_{2.5} from 2 stations (G3-B, G3-C); and PM₁₀ from one station (G3-H). Data points that were below instrument detection limits were set to 0 µg/m³ in our analysis. See Table S1 for instrument detection limits of each instrument.

The eruption period was defined as 19/03/2021 20:00 - 19/09/2021 00:00 UTC in agreement with Barsotti et al., 2023. The background period was defined differently for SO₂ and PM. For SO₂, the background period was defined as 19/03/2020 00:00 - 19/03/2021 19:00 UTC, i.e. one full calendar year before the eruption. Outside of volcanic eruption periods, SO₂ concentrations are generally low with little variability in the Icelandic atmosphere due to an absence of other sources, as shown by previous work (Carlsen et al., 2021a; Ilyinskaya et al., 2017), and subsequently confirmed by this study. The only exception is in the vicinity of aluminium smelters where relatively small pollution episodes occur periodically. A one-year long period was therefore considered as representative of the background SO₂ fluctuations. We checked our background dataset against a previous comparable in Iceland that used the same methods (Ilyinskaya et al., 2017) and found no statistically-significant difference.

PM background concentrations in Iceland are much higher and more variable than SO₂. PM frequently reaches high levels in urban and rural areas and there are significant seasonal variations (Carlsen and Thorsteinsson, 2021); the causes of this variability are discussed in the Results and Discussion. To account for this variability, we downloaded PM data for as many non-eruptive years as records existed, and analysed only the period 19 March 20:00 – 19 September 00:00 UTC in each year, i.e. the period corresponding to the calendar dates and months of the 2021 eruption. From here on, we refer to this period as ‘annual period’. The annual periods in 2010, 2011, 2014 and 2015 were partially or entirely excluded from the non-eruptive background analysis due to eruptions in other Icelandic volcanic systems (Eyjafjallajökull 2010, Grímsvötn 2011, Holuhraun 2014-2015) and associated post-eruptive emissions and/or ash resuspension. The annual period of 2022, i.e. the year following the 2021 eruption, was partially included in the background analysis: measurements between 19 March 2022 and 1 August 2022 were included, but measurements from 2 August 2022 were excluded because another eruptive episode started in Fagradalsfjall volcanic system on that date. Since August 2022 there have been 8 more eruptions in the same area at intervals of weeks-to-months, and therefore we have not included more recent non-eruptive background data. Although the 2022 annual period is only partially complete, it was particularly important for statistical analysis of PM₁ because operational measurements of this pollutant began only in 2020. The number of available background annual periods for PM₁₀ and PM_{2.5} varied depending on when each station was set up, between 1 and 12 stations with an average of 6 (Table S1).

We considered whether the year 2020 had lower PM and PM concentrations compared to other non-eruptive years because of COVID-19 pandemic societal restrictions and the extent to which this was likely to impact our results. The societal restrictions in Iceland were relatively light, for example, schools and nurseries remained opened throughout. We found that the average 2020 PM₁₀ and PM_{2.5} concentrations fell within the max-min range of the pre-pandemic years for all stations



except at G3-E where PM_{10} was 10% lower than minimum pre-pandemic annual average, and $PM_{2.5}$ was 12% lower; and at G5-A where $PM_{2.5}$ was 25% lower (no difference in PM_{10}). G3-E is at a major traffic junction in central Reykjavík, and G5-A is on a major commuter route to the capital area. For PM_1 , only 1 station was already operational in 2020 (G3-A); PM_1 concentrations at this station were 20% higher in 2020 compared to 2022 (post-pandemic). We concluded that PM data from 2020 should be included in our analysis but we do point out the potential impact of pandemic restrictions in the discussion where applicable.

2.4 Data analysis

We organised the air quality stations into geographic clusters to assess air quality by region. The geographic clusters are the immediate vicinity of the eruption site (G1, 0-4 km distance from the eruption site), the Reykjanes peninsula (G2, 9-20 km distance), the capital area of Reykjavík (G3, 25-35 km distance), Southwest Iceland (G4, 45-55 km distance), Hvalfjörður (G5, 50-55 km distance), North Iceland (G6-A ~280 km, G6-B and C ~330 km distances), and East Iceland (G7, ~400 km distance)(Fig. 1). Appendix B Figs. B1-B7 show SO_2 time series data for each individual station in geographic clusters G1-G7, respectively. Appendix B Figs. B8, B9, B10 show PM time series data for each individual station in geographic clusters G3, G5 and G6, respectively.

For each station that had data for both the eruption and background periods (SO_2 and PM), two-sample t-tests were applied to test whether the background and eruption averages were statistically significantly different for the different pollutant species.

We then calculated the number of events where pollutant concentrations exceeded current air quality thresholds and guidelines. For SO_2 , we used the ID hourly-mean threshold of $350 \mu g/m^3$ used by the (Icelandic Directive, 2016). For PM_{10} we used the ID / World Health Organisation (WHO) daily-mean threshold of $50 \mu g/m^3$ (Icelandic Directive, 2016), and for $PM_{2.5}$ we used the WHO daily-mean threshold of $15 \mu g/m^3$ (World Health Organization, 2021), as no ID threshold is defined.

There are currently no evidence-based air quality thresholds available for PM_1 . However, the Environmental Agency of Iceland uses a ‘yellow’ threshold for PM_1 at $13 \mu g/m^3$ when visualising data from the reference-grade stations and this value was used here (‘EAI threshold’).

To be able to meaningfully compare the frequency of air quality threshold exceedance events for PM_{10} , $PM_{2.5}$ and PM_1 (50, 15 and $13 \mu g/m^3$, respectively) between the eruption and the non-eruptive background periods we normalised the number of exceedance events, as explained below. This was done because the eruption covered only one annual period (see the definition of ‘annual period’ in 2.3) but the number of available background annual periods varied between stations depending on how long they have been operational, ranging between 1 and 12 periods. We normalised by dividing the total number of exceedance events at a given station by the number of annual periods at the same station. For example, for a station where the non-eruptive background was 6 annual periods the total number of exceedance events was divided by 6 to give a normalised annual number of exceedance events. The eruption covered one annual period and therefore did not require dividing. We refer to this as ‘normalised number of exceedance events’ in the Results and Discussion. Table S1



contains summary statistics for all analysed pollutant means, maximum concentrations, number of air quality threshold exceedances, and number of background annual periods for PM data.

Three reference-grade stations within geographic cluster G3 (Reykjavík capital area) measured all three PM size fractions (PM₁, PM_{2.5} and PM₁₀), which allowed us to calculate the relative contribution of different size fractions to the total PM concentration. Since PM size fractions are cumulative, in that PM₁₀ contains all particles with diameters below $\leq 10 \mu\text{m}$, the size modes were subtracted from one another to determine the relative concentrations of particles in the following categories: particles $\leq 1 \mu\text{m}$ in diameter, 1 - 2.5 μm in diameter and 2.5 - 10 μm in diameter. The comparison of size fractions between the eruption and the background was limited by the relatively short PM₁ timeseries and our results should be re-examined in the future when more non-eruptive measurements have been obtained.

3 Results and discussion

3.1 Eruption-driven increase in PM₁ concentrations relative to PM₁₀ and PM_{2.5}

Timeseries of PM₁, PM_{2.5} and PM₁₀ concentrations were collected at 3 stations in Reykjavík capital (G3-A, G3-D and G3-G, Fig. 1), allowing us to compare the relative contributions of the three size fractions in this area (25-35 km distance from the eruption site). There was a measurable change during the eruption period compared to the background, with an increase in PM₁ mass proportion relative to PM₁₀ and PM_{2.5} at all 3 stations (Fig. 2). The proportion of PM₁ mass within PM₁₀ increased from 14% in the background to 21-24% during the eruption; and from 23-44% background to 52-57% during the eruption period within PM_{2.5}. The change in proportion of PM_{2.5} within PM₁₀ was not as clear, and varied considerably between the stations. Two stations recorded a modest increase in PM_{2.5} relative to PM₁₀, from 32% background to 37-42% during the eruption period, but the third station recorded a decrease from 60% to 44%.

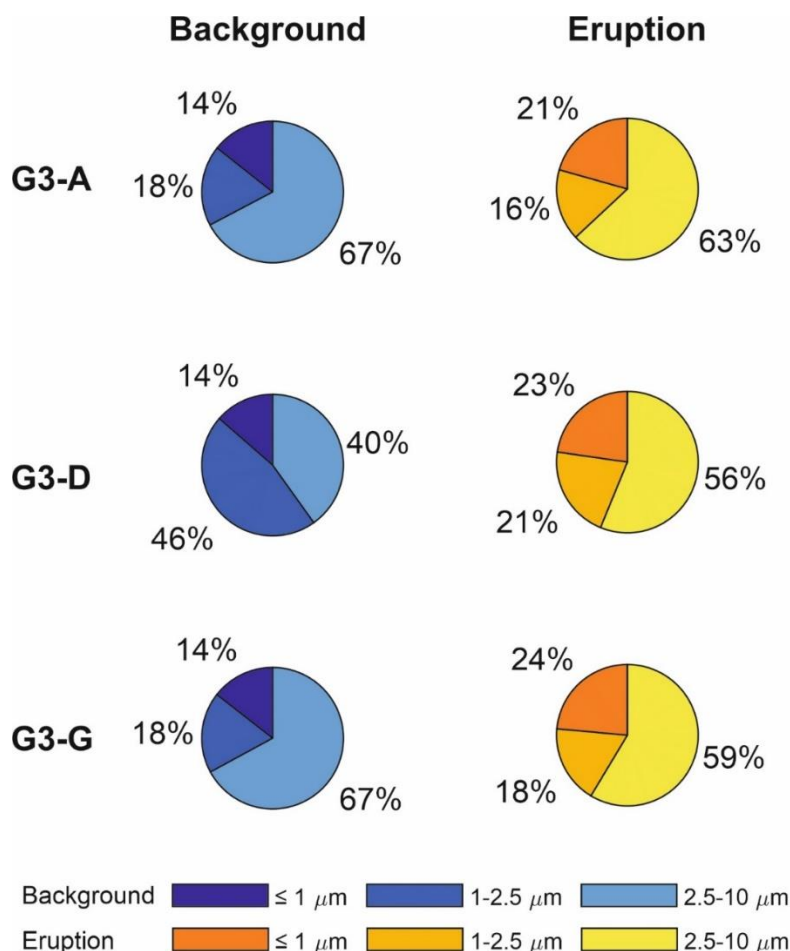


Figure 2: Relative contribution (in mass%) of three PM size fractions within PM₁₀ during the non-eruptive background and during the eruption: PM ≤ 1 μm in diameter, PM 1 - 2.5 μm in diameter and PM 2.5 - 10 μm in diameter. G3-A, G3-D and G3-E were the 3 stations in Iceland where all 3 size fractions were measured (all within Reykjavík capital area)

230 This is a novel result showing that volcanic plumes contribute a significantly higher proportion of PM₁ relative to both PM₁₀ and PM_{2.5} when sampled distally from the source (25-35 km in this study). When sampled at the active vent, volcanic plumes from basaltic fissure eruptions have previously been shown to contain a large amount of PM₁, but also a substantial proportion of coarse PM (> 2.5 μm) (Ilyinskaya et al., 2017; Martin et al., 2011; Mason et al., 2021). At-vent, the composition of the fine and coarse size modes is typically very different, with the finer fraction formed via the conversion of

235 SO₂ gas into sulphate particles, and the coarser fraction made of fragmented silicate material (i.e. ash, which is found in some small concentrations even in typically ash-poor eruptions) (Ilyinskaya et al., 2021). The conversion of SO₂ gas to sulphate particles continues for hours and days after emission from the volcanic vents forming new quantities of fine particles (Green et al., 2019; Pattantyus et al., 2018), while ash particles are not renewed in the plume after emission and are progressively lost through deposition. This can explain the elevated concentrations of particles in the finer size fractions

240 observed downwind of the eruption site relative to the other size fractions. This finding has an implication for the health



hazards posed by volcanic plumes in populated areas, which are typically located at a distance of tens-hundreds of kilometers from the eruption site.

3.2 Significant but small increases in average pollutant levels

Most areas of Iceland, up to 400 km distance from the eruption site, recorded a small but statistically significant increase in average SO₂ and PM concentrations during the eruption compared to the background period.

Figure 3 and Table 1 compare SO₂ concentrations (hourly-means, µg/m³), measured by reference-grade stations across Iceland. During the non-eruptive background period, SO₂ concentrations were low (long term hourly-mean average generally <2 µg/m³), which is in agreement with previous studies (Ilyinskaya et al., 2017). Stations in the vicinity of aluminium smelters (G5-1 and 2, G6-C and G7-all) had higher long-term average values and periodically measured short-lived escalations in SO₂ hourly-mean concentrations of several 10s or 100s of µg/m³ during the background period (Fig. 3, Table 1 and Table S1). Station G7-D (East Iceland at ~400 km distance from the eruption site) was the only one where the eruption-related increase in average SO₂ concentrations was below statistical significance. This station was in a vicinity of an aluminium smelter, and was also missing over 1/3 of the eruption period data due to technical issues, which may have reduced the observed eruption impact.

The average SO₂ concentrations were higher during the eruption at all reference-grade stations that had data from both before and during the eruption ($n=16$), and the increase was statistically significant ($p<0.05$) at 15 out of the 16 stations. Across all 7 geographic clusters, the absolute increase in average SO₂ concentrations between the background and eruption period was relatively low, on the order of a few µg/m³ (Fig. 3 and Table 1). For example, the average concentration across Reykjavík capital changed from 0.32 µg/m³ in the background to 4.1 µg/m³ during eruption.

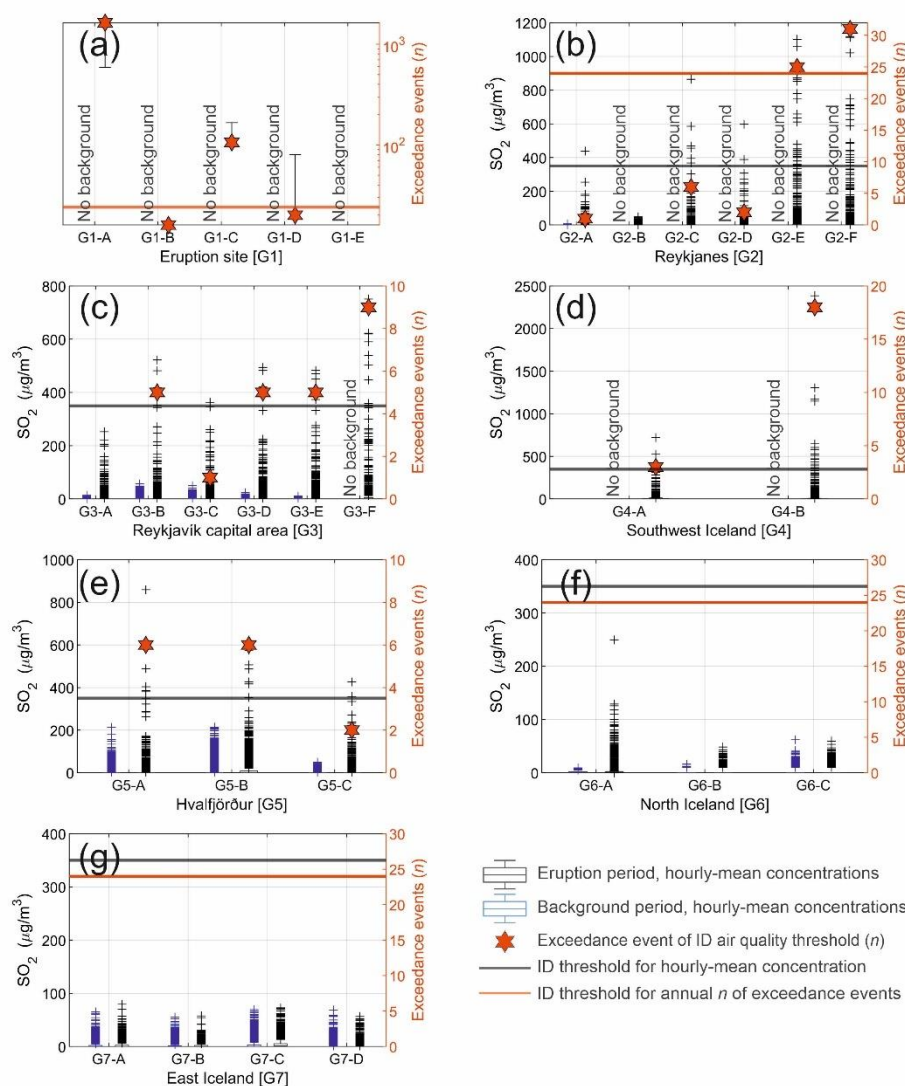
The absolute increases in average PM concentrations in all measured size fractions were relatively modest, similar to the change observed in SO₂ average concentrations. Table 2 and Figs. 4-6 show PM₁₀, PM_{2.5} and PM₁ concentrations (daily-means, µg/m³) measured in the 3 geographic area where reference-grade monitoring was available. For example, in Reykjavík capital (at stations where concentrations during the eruption period were statistically-significantly higher than background), the average PM₁₀ concentration changed from 9-10 µg/m³ in the background to 12-13 µg/m³ during the eruption period; average PM_{2.5} from 3-4 µg/m³ background to ~5 µg/m³ eruption; and average PM₁ from 1.3-1.5 µg/m³ background to ~3 µg/m³ eruption (Fig. 4).

Table 1: SO₂ concentrations (hourly-mean, µg/m³) in populated areas around Iceland during the non-eruptive background and during the Fagradalsfjall 2021 eruption. ‘Average’ is the average hourly-mean of all stations within a geographic area. ‘Peak’ is the maximum hourly-mean recorded by an individual station within the geographic area. ‘ID exceedances’: number of times that the SO₂ concentrations exceeded the Icelandic Directive air quality threshold of 350 µg/m³. Number of AQ exceedances is the maximum number of exceedances recorded by an individual station within a geographic area.

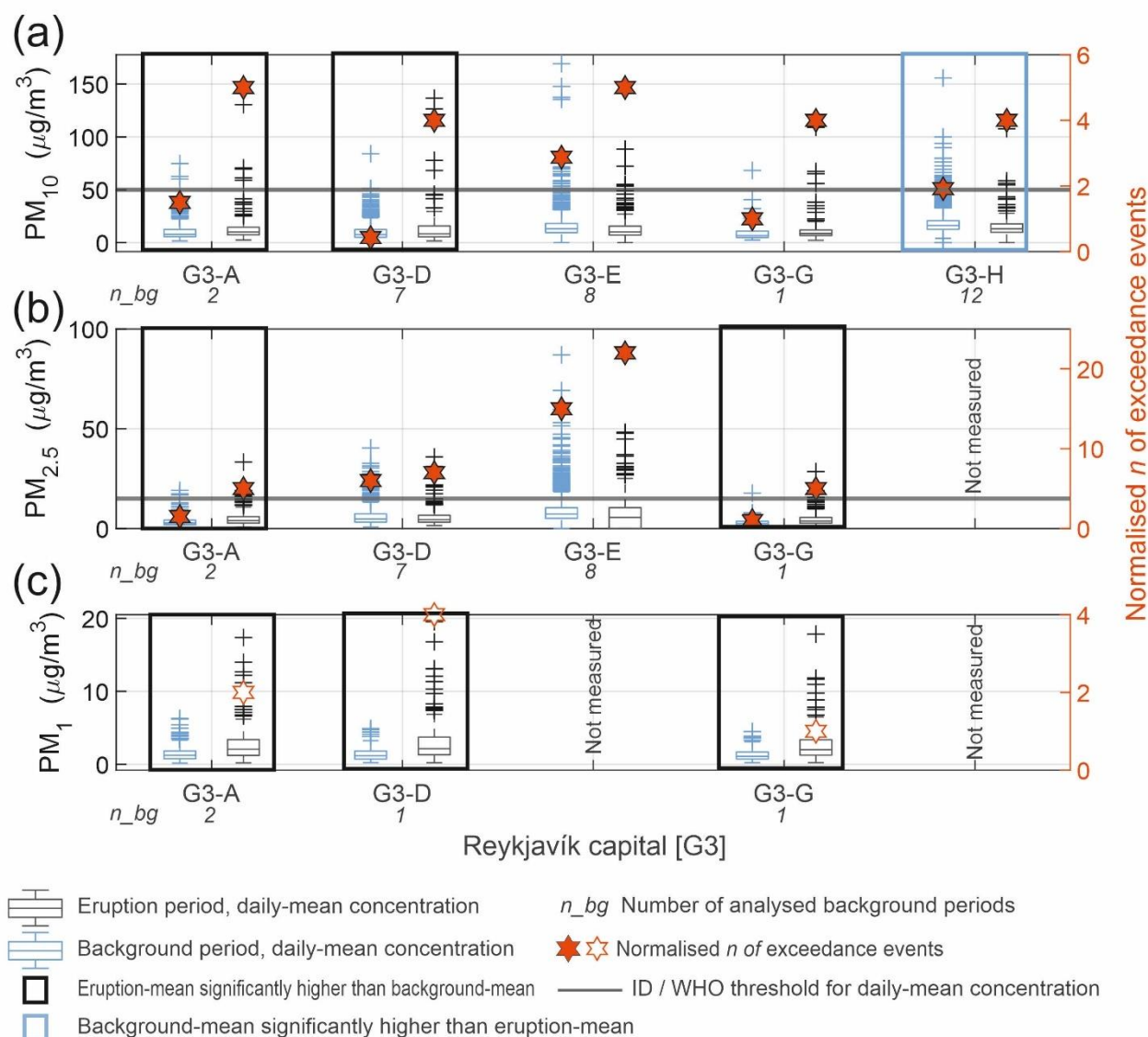
Geographic	N	of	Distance	SO ₂ hourly-mean (µg/m ³)				ID exceedances (max n)	
				Background	Eruption	Background	Eruption	Background	Eruption



area	stations	from eruption site (km)	average	average	peak	peak		
Reykjanes peninsula (G2)	6	9-20	0.14	4.6	7.7	2400	0	31
Reykjavík capital (G3)	6	25-35	0.32	4.1	57	750	0	9
South Iceland (G4)	2	45-55	No data	6.1	No data	2400	No data	18
Hvalfjörður (G5)	3	50-55	3.8	8.2	210	860	0	6
North Iceland (G6)	3	280-330	0.38	1.7	9.1 at 280 km; 62 at 330 km	250 at 280 km; 48 at 330 km	0	0
East Iceland (G7)	4	400	1.8	2.4	69	79	0	0



275 **Figure 3: Hourly-mean concentrations and number of ID threshold exceedance events for SO₂ (µg/m³), measured by 29 stations**
 across 7 geographical areas in Iceland (a-g). The data are shown as box-and-whiskers plots, with crosses representing extremely
 high values (statistical outliers). Pre-eruptive background is shown for stations that were in operation before the eruption started.
 Panel (a) shows eruption-site measurements collected by lower-accuracy sensors for which we only report number of exceedances
 of the ID air quality threshold (350 µg/m³). Panels (b-g) show data from reference-grade stations in populated areas as SO₂ hourly-
 mean concentrations and the number of exceedance events. The ID air quality threshold of 350 µg/m³ hourly-mean is shown on all
 panels with a black horizontal line. The figure also shows whether the number of threshold exceedances at each station exceeded
 the recommended annual total (n=24, orange horizontal line). Note logarithmic scale for Eruption site (a). Time series plots for
 each station are available in Appendix B Figures B1-B7.



285 **Figure 4: Daily-mean concentrations of (a) PM_{10} , (b) $PM_{2.5}$ and (c) PM_1 ($\mu g/m^3$), measured in Reykjavík capital area. The**
 concentrations are shown as box-and-whiskers plots, with crosses representing extremely high values (statistical outliers). Pre-
 eruptive background is shown for stations which were in operation before the eruption started, n_{bg} indicates the number of
 background annual periods for each station (see Methods for definition of a background annual period). Stations where the
 average concentration during the eruption period was statistically-significantly higher than the background are highlighted with a
 290 black box. Stations where the average concentration during the eruption period was statistically-significantly lower than the
 background are highlighted with a blue box. Absence of a box indicates no significant difference between eruption and
 background periods. The figure shows the normalised number of times PM_{10} and $PM_{2.5}$ concentrations at each station exceeded
 the ID air quality threshold of 50 and 15 $\mu g/m^3$ daily-mean, respectively. For PM_1 , the figure shows the number of times the
 concentration during the eruption exceeded the EAI threshold of 13 $\mu g/m^3$ daily-mean. The number of threshold exceedance
 295 events is normalised to the length of the measurement period – refer to the main text for an explanation of the method. Time series
 plots for each station are available in Appendix B Figure B8.

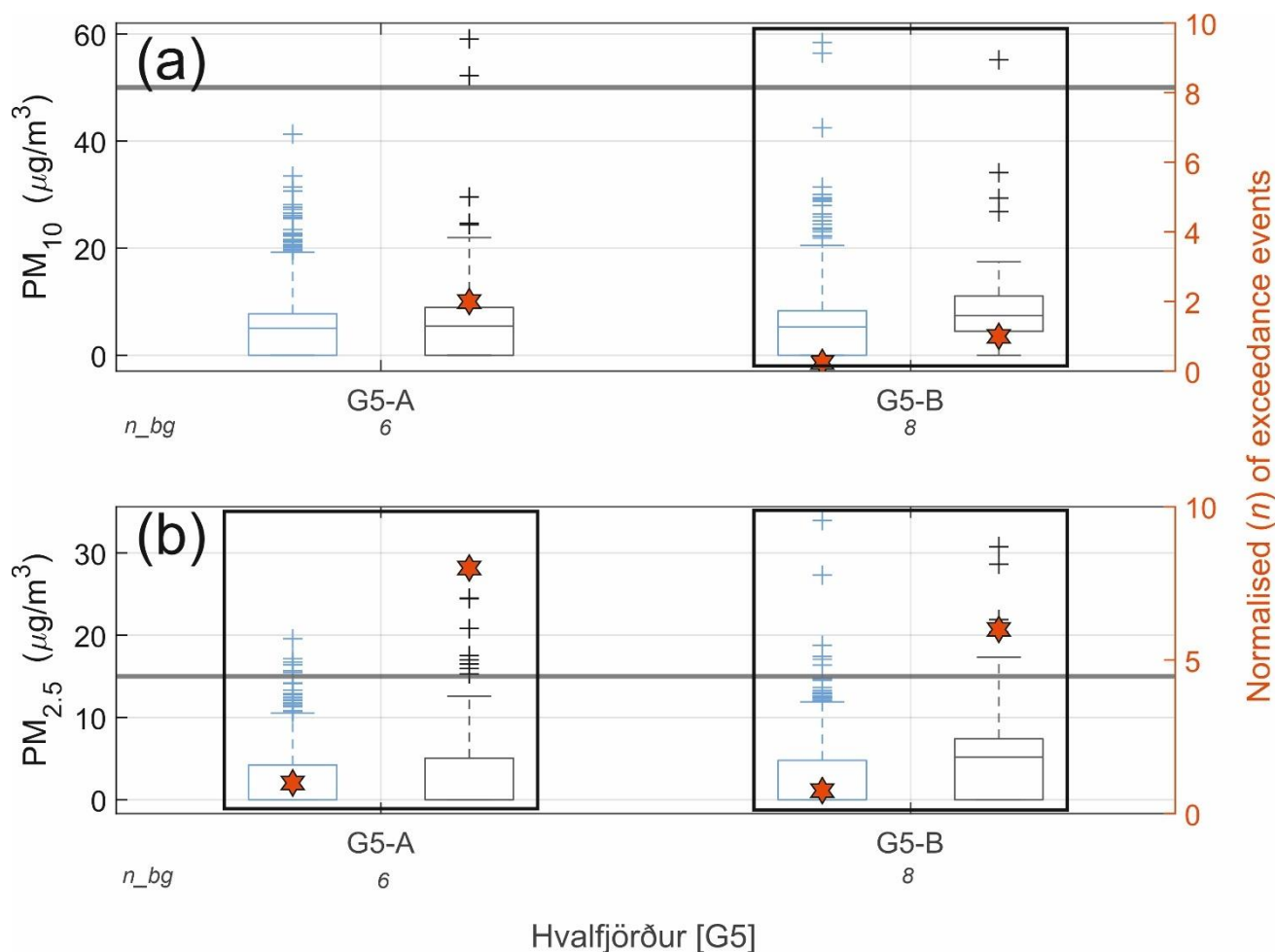


Figure 5: Daily-mean concentrations of (a) PM_{10} , and (b) $\text{PM}_{2.5}$ ($\mu\text{g}/\text{m}^3$), measured in Hvalfjörður area. The concentrations are shown as box-and-whiskers plots, with crosses representing extremely high values (statistical outliers). Pre-eruptive background is shown for stations which were in operation before the eruption started, n_{bg} indicates the number of background annual periods for each station (see methods for definition of a background annual period). Stations where the average concentration during the eruption period was statistically-significantly higher than the background are highlighted with a black box (absence of a box indicates no significant difference). The figure shows the normalised number of times PM_{10} and $\text{PM}_{2.5}$ concentrations at each station exceeded the ID air quality threshold of 50 and 15 $\mu\text{g}/\text{m}^3$ daily-mean, respectively. The number of threshold exceedance events is normalised to the length of the measurement period – refer to the main text for an explanation of the method. Time series plots for each station are available in Appendix B Figure B9.

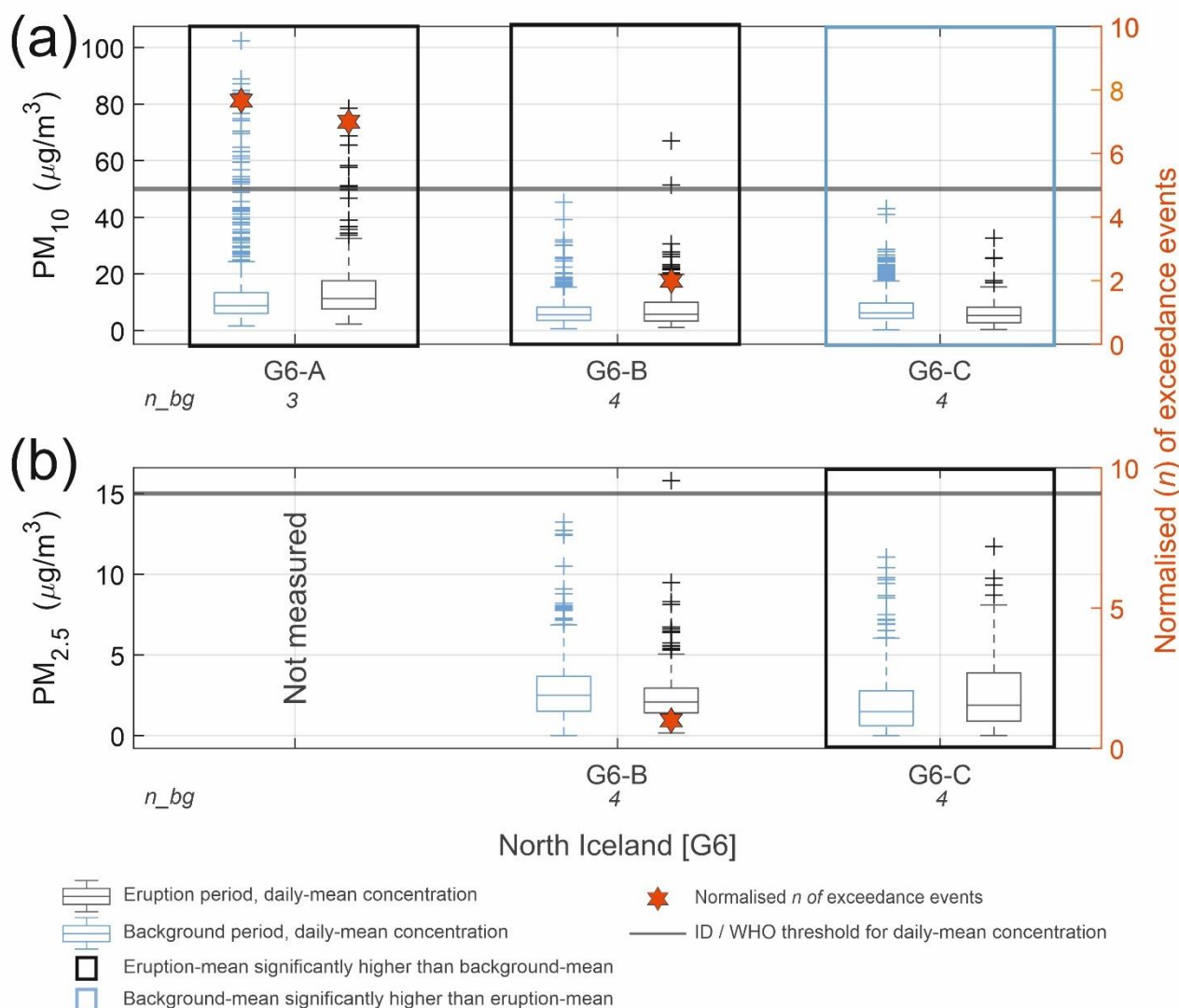


Figure 6: Daily-mean concentrations of (a) PM_{10} , and (b) $PM_{2.5}$ ($\mu g/m^3$), measured in North Iceland. The concentrations are shown as box-and-whiskers plots, with crosses representing extremely high values (statistical outliers). Pre-eruptive background is shown for stations which were in operation before the eruption started, n_{bg} indicates the number of background annual periods for each station (see methods for definition of a background annual period). Stations where the average concentration during the eruption period was statistically-significantly lower than the background are highlighted with a blue box. Absence of a box indicates no significant difference between eruption and background. The figure shows the normalised number of times PM_{10} and $PM_{2.5}$ concentrations at each station exceeded the ID air quality threshold of 50 and 15 $\mu g/m^3$ daily-mean, respectively. The number of threshold exceedance events is normalised to the length of the measurement period – refer to the main text for an explanation of the method. Time series plots for each station are available in Appendix B Figure B10.



320

Table 2 PM₁₀, PM_{2.5} and PM₁ concentrations (µg/m³, 24-h mean) in populated areas around Iceland during the non-eruptive background ('b/g') and during the Fagradalsfjall 2021 eruption ('erupt.'). 'Average' is the average 24 h-mean of all stations within the geographic area. 'Peak' is the maximum 24 h-mean recorded by an individual station within a geographic area. 'AQ exceedances' is number of times that the PM concentrations exceeded the following concentrations: PM₁₀ 50 µg/m³ 24 h-mean; PM_{2.5} 15 µg/m³ 24 h-mean; PM₁ 13 µg/m³ 24h-mean. 'AQ exceedances' is the maximum number of exceedances recorded by an individual station within a geographic area.

			PM ₁₀						PM _{2.5}						PM ₁					
			Average (µg/m ³ , 24- h mean)		Peak (µg/m ³ , 24- h mean)		AQ exceedance s (max <i>n</i>)		Average (µg/m ³)		Peak (µg/m ³ , 24- h mean)		AQ exceedance s (max <i>n</i>)		Average (µg/m ³ , 24- h mean)		Peak (µg/m ³ , 24- h mean)		AQ exceedance s (max <i>n</i>)	
Geograph ic area	<i>n</i> of statio ns (PM1 0, PM2. 5, PM1)	Distan ce from eruptio n site (km)	B/ G	Erup t.	B/ G	Erup t.	B/ G	Erup t.	B/ G	Erup t.	B/ G	Erup t.	B/ G	Erup t.	B/ G	Erup t.	B/ G	Erup t.	B/ G	Erup t.
Reykjaví k capital (G3)	5, 4, 3	25-35	11	13	17 0	140	2.9	5	4.6	5.3	87	48	15	22	1.4	2.8	6.3	20	0	4
Hvalfjörð ur (G5)	3	50-55	5.7	7.6	58	59	0.2 5	2	2.1	4.2	34	31	1	8	No data					
North Iceland (G6)	3	280- 330	8.1	8.6	10 0	79	7.7	7	0.5 3	0.72	13	16	0	1						

325



Generally, PM_1 and $PM_{2.5}$ showed a more consistent eruption-related increase than PM_{10} , which agrees with our results on their relative proportions discussed in 3.1. During the eruption, PM_1 average concentrations were statistically-significantly higher at all monitored stations in Reykjavík capital (G3, Fig. 4). The $PM_{2.5}$ and PM_{10} concentrations were statistically-significantly higher during the eruption at approximately half of the monitored stations across all geographic stations (Figs. 4-6). The locations that recorded significant eruption-related increases in average PM_{10} and $PM_{2.5}$ concentrations generally had lower non-eruptive background concentrations. The stations with higher background PM_{10} and $PM_{2.5}$ were generally located closer to roads with heavy traffic; this shows that local sources such as road traffic were more important PM_{10} and $PM_{2.5}$ pollution sources than the distal eruption, but the eruption impacts on average levels of PM_{10} and $PM_{2.5}$ were more noticeable in areas with lower background concentrations. Average levels of PM_1 were unequivocally higher during the eruption period compared to the background, but this pollutant was only monitored in the Reykjavík capital area. It remains to be investigated whether volcanic contribution to PM_1 would also dominate over other sources in more distal communities.

3.3 Impact on pollutant peak concentrations and number of air quality exceedance events

Unlike the modest (or, at some stations, negligible) increases in the average concentrations of PM and SO_2 , the eruption was associated with large increases in the number of air quality threshold exceedance events in the near- and far-field.

Figure 3 and Table 1 compare the background and the eruption periods with respect to peak concentrations, and the number of Iceland Directive (ID) threshold exceedance events for SO_2 ($350 \mu g/m^3$ hourly-mean). During the non-eruptive background the SO_2 concentrations never exceeded the ID threshold at any of the stations. During the eruption, the numbers of threshold exceedance events ranged between 0 and 31 at individual stations and were, broadly speaking, the highest closer to the eruption site (Fig. 3 and Table 1). However, there were noticeable fine-scale spatial variations in SO_2 concentrations within individual geographical areas as discussed further in 3.4. The ID threshold for total annual hourly-mean exceedances ($n=24$) was exceeded in the geographic cluster in the immediate vicinity of the eruption site (G1; up to 1600 events at an individual station), and in two communities on the Reykjanes peninsula (G2; 25 and 31 events, respectively). We attributed the combination of a relatively low absolute increase in the average SO_2 concentrations, and a large increase in peak concentrations to a combination of the pulsating behaviour of the eruption emissions, and highly variable local meteorological conditions (wind rose for eruption site is in Appendix B Fig. B11 (Barsotti et al., 2023; Pfeiffer et al., 2024)). This meant that the volcanic plume was only periodically advected into individual populated areas, rather than being a persistent source of pollution in the same location.

PM_1 concentrations never exceeded the EAI threshold ($13 \mu g/m^3$) in the background period but during the eruption exceeded between 3 and 5 times at all stations where it was monitored (Fig. 4, Table 2). The number of PM_{10} and $PM_{2.5}$ exceedance events was higher during the eruption period at all stations in Reykjavík capital area (G3) and in Hvalfjörður (G5), and at 2 out of 3 North Iceland (G6) stations that recorded any threshold exceedances.

PM_1 peak concentrations increased from $5-6 \mu g/m^3$ peak daily-mean during the background period to $\sim 20 \mu g/m^3$ peak daily-mean during the eruption period, across all 3 monitored stations in Reykjavík capital (G3). Volcanic impact on PM_{10} and



360 $PM_{2.5}$ was more variable compared to PM_{10} . Reykjavík capital stations with cleaner PM_{10} and $PM_{2.5}$ backgrounds (peak
daily-mean $<80 \mu\text{g}/\text{m}^3$ PM_{10} and $<20 \mu\text{g}/\text{m}^3$ $PM_{2.5}$) showed larger impacts from the eruption than stations with more polluted
background conditions (peak daily-means $\geq 110 \mu\text{g}/\text{m}^3$ PM_{10} and $\geq 40 \mu\text{g}/\text{m}^3$ $PM_{2.5}$). The cleaner stations show eruption-
related increases of up to $40\text{--}60 \mu\text{g}/\text{m}^3$ PM_{10} and $10\text{--}14 \mu\text{g}/\text{m}^3$ $PM_{2.5}$ above peak background levels while the more polluted
stations did not have noticeable increases in peak daily-means of PM_{10} and $PM_{2.5}$ during the eruption. Further afield, in
365 Hvalfjörður and North Iceland (Figs. 5-6), the number of monitoring stations was too low for a statistical analysis, but
generally the same pattern was observed: stations with lower non-eruptive background PM_{10} and $PM_{2.5}$ generally recorded
increases in peak daily-mean concentrations of up to ~ 20 and $5 \mu\text{g}/\text{m}^3$, respectively, above background levels.
The statistically significant impact on average and peak PM levels observed in the Reykjavík capital and further afield (in up
to at least 300 km distance) is remarkable considering the relatively small size of the eruption and the importance of non-
370 volcanic PM sources in Iceland. In rural areas, the main non-volcanic source of PM is re-suspended natural dust sourced
from highland deserts (Butwin et al., 2019), with higher levels in the drier summer seasons. In urban areas, the non-volcanic
PM pollution peaks are typically higher in the winter with the main source being tarmac road erosion by studded tyres
(Carlsen and Thorsteinsson, 2021). The unequivocal eruption-related increase in average and peak concentrations of PM_{10}
suggests that volcanic fissure eruptions are one of, or potentially the most, important source of PM_{10} in Iceland, at least during
375 the summer months. Table 3 compares concentration ratios of the three measured PM size fractions in Reykjavík between a
representative eruption-free background; the 2021 volcanic plume; and two Icelandic desert dust storms in 2023. The
comparison is made based on a small dataset but suggests distinct ‘fingerprint’ ratios for the different pollution sources.
These ratios may be used for identifying sources of PM pollution episodes in Reykjavík and potentially other distal
populated areas, especially when the sources are difficult to identify using meteorological and/or visual observations. During
380 the winter months, the contribution of tarmac erosion by studded tyres may affect the ratios; and higher short-lived peak
concentrations may happen during New Years Eve fireworks – more data on winter-time eruptions is needed to establish
this.



Table 3. Concentration ratios of PM size fractions (hourly-means, $\mu\text{g}/\text{m}^3$) associated with different pollution sources in Reykjavík capital area. Green-coloured rows show ratios during periods considered to be representative of typical Reykjavík background: ‘Summer period’ when studded tyres are not in use (banned between 14 April and 31 October), and a period during the 2021 eruption when the plume was being advected away from Reykjavík. Orange-coloured rows show ratios during the 2021 eruption when the plume was advected to Reykjavík; for definitions of fresh and mature plume see section 3.4. ‘Desert dust’ are pollution episodes caused by Icelandic highland desert storms (source area ~200 km from Reykjavík), confirmed by IMO meteorological and visual observations. Station G3-G is listed first as it is considered to be the most sensitive one to the presence of volcanic plume due to low background concentrations from local sources.

	Start date	Start time	End date	End time	G3-G	G3-A	G3-D	G3-G	G3-A	G3-D	G3-G	G3-A	G3-D
					PM ₁ /PM ₁₀	PM ₁ /PM ₁₀	PM ₁ /PM ₁₀	PM ₁ /PM _{2.5}	PM ₁ /PM _{2.5}	PM ₁ /PM _{2.5}	PM _{2.5} /PM ₁₀	PM _{2.5} /PM ₁₀	PM _{2.5} /PM ₁₀
Summer period, no eruption	01/05/2020	00:00	01/09/2020	00:00	0.16	0.15	0.13	0.44	0.43	0.22	0.35	0.34	0.61
Eruption but no plume in Reykjavík	01/04/2021	09:00	02/04/2021	10:00	0.17	0.19	0.24	0.41	0.43	0.45	0.42	0.43	0.54
Fresh plume	18/07/2021	10:00	19/07/2021	16:00	0.65	0.68	0.7	0.9	0.92	0.84	0.72	0.73	0.78
Mature plume 1	28/04/2021	08:00	29/04/2021	20:00	0.43	0.29	0.49	0.8	0.73	0.8	0.53	0.39	0.6
Mature plume 2	19/05/2021	14:00	21/05/2021	11:00	0.71	0.65	0.85	0.96	0.95	0.95	0.73	0.68	0.89
Mature plume 3	01/07/2021	09:00	06/07/2021	08:00	0.67	0.59	0.65	0.91	0.88	0.84	0.74	0.66	0.74
Desert dust 1	03/11/2023	13:00	04/11/2023	02:00	0.02	n/a	0.02	0.11	n/a	0.13	0.15	n/a	0.15
Desert dust 2	08/11/2023	14:00	09/11/2023	00:00	0.01	n/a	0.01	0.1	n/a	0.086	0.15	n/a	0.15



3.4 Fine-scale temporal and spatial variability in SO₂ and PM₁ peaks

395 The dense reference-grade network between 9 and 35 km from the eruption site (clusters G2 and G3) revealed fine-scale variability at these relatively distal sites. Five out of 6 stations on Reykjanes peninsula (SO₂ only) were north and northwest from the eruption site, within the most common wind direction (wind rose in Fig. B11). Despite only 3-16 km distance between these stations, two of them (G2-E and G2-F) recorded 25 and 31 SO₂ hourly-mean exceedance events, respectively, while G2-B, G2-C and G2-D recorded between 0 and 6 events (Fig. 3). To test that this was not an artifact of some of the stations having been set up later than others during the eruption, we also counted the number of exceedance events from 7 May 2021, the date by which all G2 stations had become operational. The result was largely unchanged: the number of exceedance events remained higher at G2-E and F (7 and 26 events, respectively) and lower at G2-B, C, and D (0-6 events). The spatio-temporal difference between the 'high exceedance stations' G2-E and G2-F, which were within 5 km distance of each other is also noteworthy: during the first 7 weeks of the eruption (19 March – 7 May 2021) G2-E recorded 18 of its total 405 25 exceedance events, while G2-F recorded only 5 out of 31. This likely reflects the control of the wind direction rather than topography as both stations were close to sea level, and demonstrates that the edges of the volcanic pollution cloud were simply defined.

Reykjavík capital area stations (G3) were located 25-35 km from the eruption site and within <1 and 10 km from one another (Fig. 1). The most significant volcanic plume advection episode happened on 18-19 July 2021, when the G3 stations 410 cumulatively recorded 21 SO₂ hourly-mean air quality exceedance events out of the 23 recorded during the whole eruption. This advection episode revealed how the concentrations of volcanic pollutants varied on a fine spatio-temporal scale. Figures 7a-7d show the spatio-temporal resolution and ratios of SO₂ and PM as hourly-means during this episode. We focus this discussion on PM₁ rather than PM_{2.5} and PM₁₀ because PM₁ more clearly represented the volcanic source compared to the other size fractions, as discussed in 3.1 and shown on Figs. 7c-7d. Both SO₂ and PM₁ were highly elevated above 415 background concentrations during the advection episode at all G3 stations (Figs. 7a-7d). Stations G3-A and G3-E were located < 1 km of each other; during the 18-19 July episode G3-E recorded ~2 times higher maximum SO₂ concentrations than G3-A (480 and 250 µg/m³, respectively), and five SO₂ air quality threshold exceedance events while G3-A recorded zero (Figs. 2 and 7a). The fine scale spatio-temporal differences were also observed in PM₁: for example, G3-D recorded up to twice as high PM₁ hourly-means than G3-G during the same advection episode (Fig. 7b). The topographic elevation 420 difference between G3 stations is unlikely to explain the spatial fluctuations as it is relatively small. Most of the G3 stations are located between 10 and 40 m above sea level (a.s.l.) and G3-F is at 85 m a.s.l.. One potential contributing factor could be channelling and/or downwash of air currents by urban buildings, a process that might be important for central Reykjavík locations, and requires further investigation, e.g. by fine-scale dispersion modelling, but is beyond the scope of this study. The relative proportions of the two pollutants, SO₂ and PM₁, in the 18-19 July advection episode varied strongly between the 425 two stations that measured both of them (G3-A and G3-D). The SO₂ peak hourly-mean differed by nearly a factor of 2 between the two stations (Fig. 7a); but PM₁ peak hourly-means only by a maximum of 20% (Fig. 7b). During the advection



episode, both pollutants showed 3 principal concentration peaks. The first of the three principal concentration peaks (July 18 13:00) recorded the highest SO₂ concentration at station G3-D, and the last of the 3 pollution peaks (July 19 23:00) recorded the highest PM₁ concentration at the same station (Figs 7a-7b).

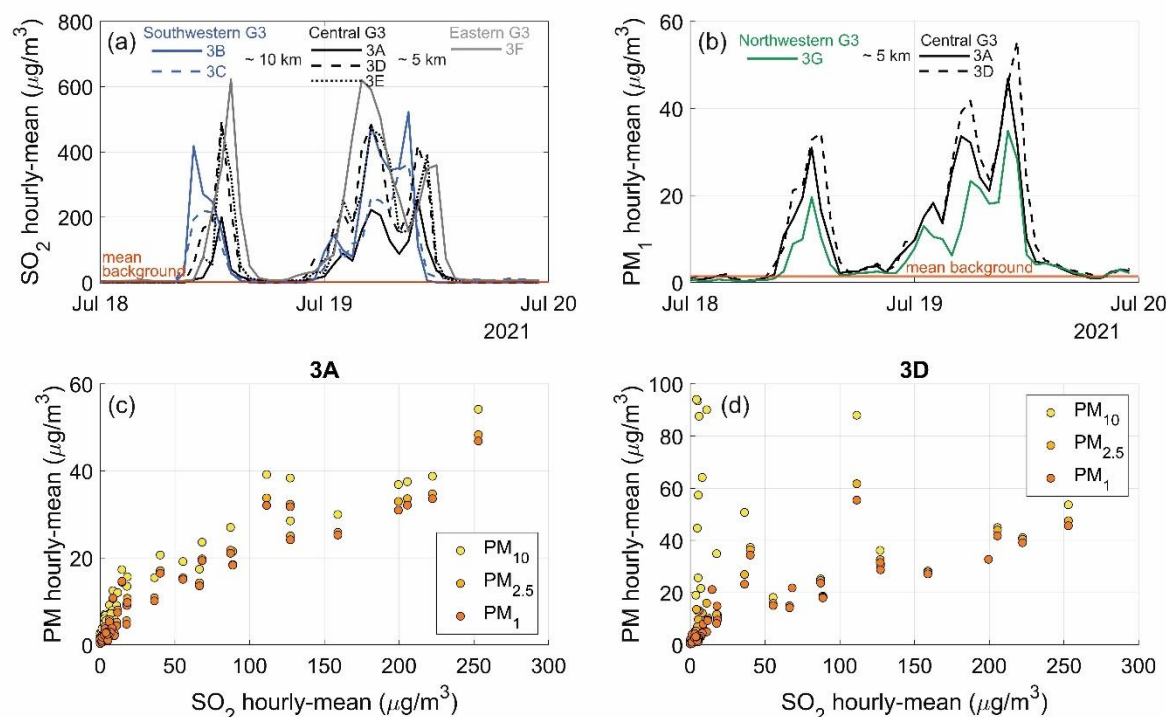


Figure 7: SO₂ and PM concentrations ($\mu\text{g}/\text{m}^3$) during a 'fresh' volcanic plume advection episode in Reykjavík capital area (G3) 18-19 July 2021. 3A to 3F are names of reference-grade stations and the figure indicates their respective locations within Reykjavík (southwestern, central, eastern, and northwestern) and the approximate distance between them. Panel (a): SO₂ hourly-means timeseries. Panel (b): PM₁ hourly-means timeseries. Panel (c): Scatter plot between concentrations of SO₂ and PM₁₀, PM_{2.5} and PM₁ at station 3A, which measured all of these pollutants. Panel (d): Scatter plot between concentrations of SO₂ and PM₁₀, PM_{2.5} and PM₁ at station 3D, which measured all of these pollutants.

We also examined the fluctuations in SO₂ and PM₁ during an advection episode of a chemically mature plume locally known as 'móða', or 'vog' in English (volcanic smog) in Reykjavík capital area July 1-7 2021 (Fig. 8a-8d). A chemically mature plume has undergone significant gas-to-particle conversion of sulphur in the atmosphere and, as shown by Ilyinskaya et al. (2017), may be advected into the populated area some days after the initial emission. The mature plume (Figs. 8c-8d) has a higher PM/SO₂ ratio than a fresh plume (Figs. 7c-7d), and SO₂ is elevated to above-background levels to a variable degree, sometimes only slightly (Ilyinskaya et al., 2017). Conditions which would typically facilitate the generation of móða and its accumulation are low wind speed, high humidity and intense solar radiation. Based on these factors, the 1-7 July episode was identified by IMO at the time of the event as móða, and a public air quality advisory was issued. Figs. 8c-8d shows that



during the móða event PM_{10} is frequently elevated without a correspondingly-high increase in SO_2 . The highest peaks of SO_2 were well-defined but PM_{10} was highly elevated above background levels throughout the whole period with less prominent individual concentration peaks. It is possible that PM_{10} grounds more persistently than SO_2 , which could be tested in follow-on work by dispersion modelling with high vertical resolution near ground level.

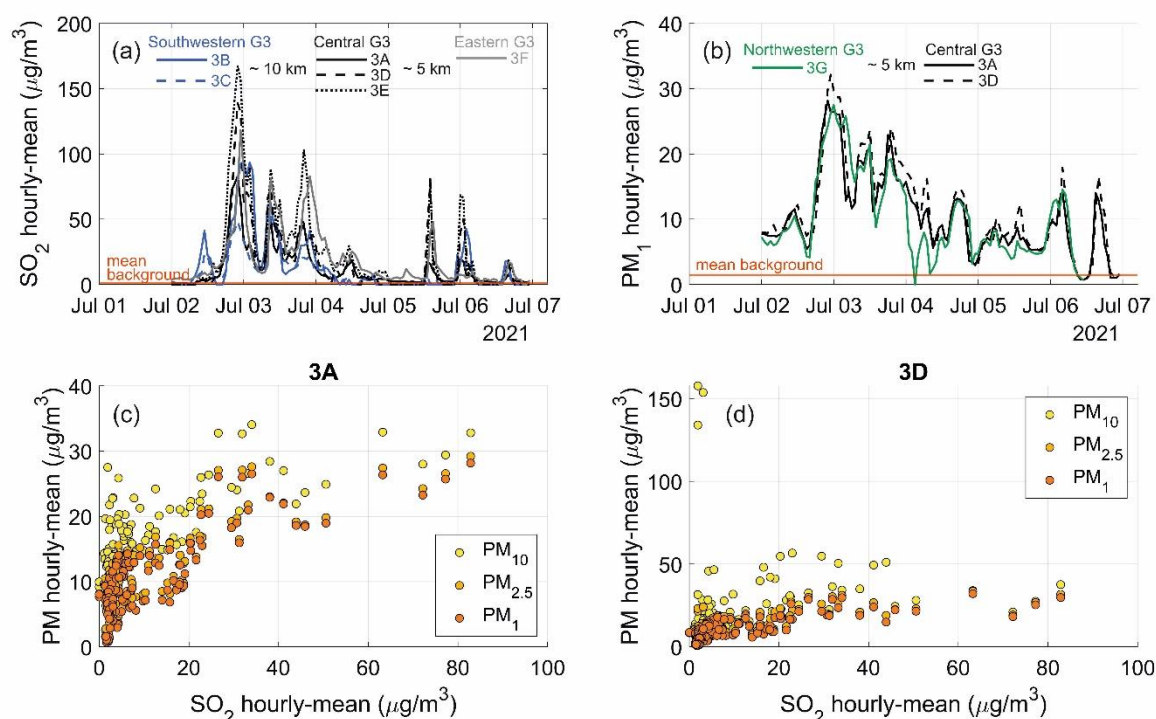


Figure 8: SO_2 and PM concentrations ($\mu g/m^3$) during a ‘mature’ volcanic plume advection episode in Reykjavik capital area (G3) 1-7 July 2021. 3A to 3F are names of reference-grade stations and the figure indicates their respective locations within Reykjavik (southwestern, central, eastern, and northwestern) and the approximate distance between them. Panel (a): SO_2 hourly-means timeseries. Panel (b): PM_{10} hourly-means timeseries. Panel (g): Scatter plot between concentrations of SO_2 and PM_{10} , $PM_{2.5}$ and PM_1 at station 3A, which measured all of these pollutants. Panel (h): Scatter plot between concentrations of SO_2 and PM_{10} , $PM_{2.5}$ and PM_1 at station 3D, which measured all of these pollutants.

3.5 Potential population exposure to volcanic air pollution

3.5.1 Exposure of residents

We considered the frequency of exposure in populated areas to SO_2 levels above air quality thresholds ($350 \mu g/m^3$ hourly-mean). Evidence-based air quality thresholds for PM_{10} do not yet exist, however, as shown in previous sections (e.g. Figs. 7 and 8), volcanic advection episodes contained SO_2 , PM_{10} and $PM_{2.5}$ (and to a less significant extent, PM_1) and therefore people exposed to elevated levels of volcanic SO_2 were most likely also exposed to elevated levels of fine PM.



Data on the Icelandic population in the year 2020 were obtained from Statistics Iceland (2022) and were considered representative for 2021. Population data were obtained for each municipality of Iceland, both the total municipality population as well as population by age demographics. In 2020, Iceland had a population of 369,000. Of the total population, 6% and 15% of the population were in the age groups of ≤ 4 and ≥ 65 years, respectively, which have been shown to be more vulnerable to volcanic air pollution (Carlsen et al., 2021b, a). There were 263,000 people, equating to 71% of the total population, within 50 km of the Fagradalsfjall eruption site where most of the SO_2 air quality threshold exceedances occurred. Fig. 9 shows municipality-level population data for this area, number of vulnerable age-group individuals, location of hospitals, and the number of ID air quality threshold exceedances at monitoring stations.

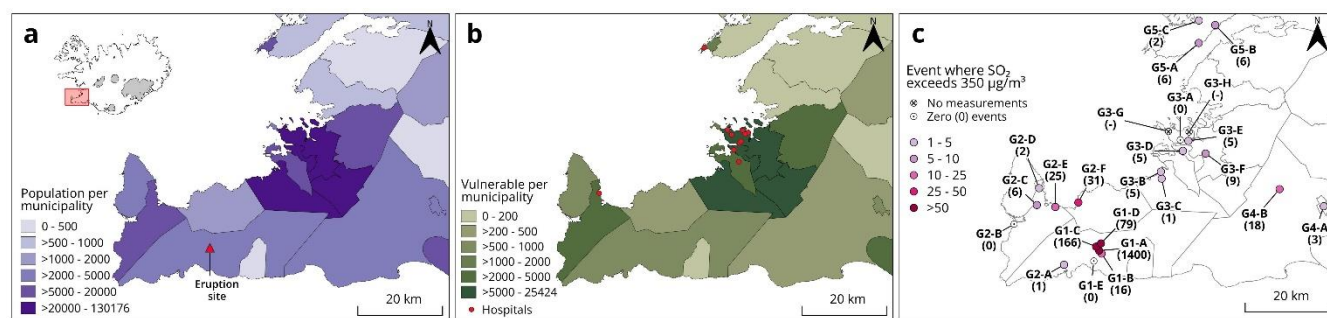


Figure 9: Potential exposure of the general population of Iceland to above-threshold SO_2 concentrations ($350 \mu\text{g}/\text{m}^3$ hourly-mean). Panel (a): Population map at the municipality level of the densely populated southwestern part of Iceland, including the Reykjavík capital area (area G3). Population data in this figure for 2020 from Statistics Iceland. Panel (b): Map of potentially vulnerable sub-populations (≤ 4 years and ≥ 65 years of age) in each municipality. Location of hospitals is shown. Panel (c): Number of events when SO_2 concentrations exceeded the ID air quality threshold of $350 \mu\text{g}/\text{m}^3$ hourly-mean during the eruption period as measured by the monitoring stations (areas G1, G2 and G3). Source and copyright of basemap and cartographic elements: Icelandic Met Office & Icelandic Institute of Natural History.

The capital area had 210,000 residents (60% of the total population), a high density of individuals in the more-vulnerable age groups and a large number of hospitals (area G3 on Fig. 9). Air quality stations in the densely-populated capital area recorded between 0 and 9 threshold exceedance events. The fine-scale spatial differences in ground-level pollutant concentrations (section 3.4) were potentially very important for the total exposure. For example, one of the largest hospitals in the country was located equidistantly (~ 2 km) from stations G3-A and G3-E that recorded, respectively, 0 and 5 SO_2 exceedance events, so it is not known how frequently people at the hospital were exposed to above-threshold levels. Similarly, the hospital closest to the eruption site (~ 10 km distance) was located in between two air quality monitoring stations (G2-D and G2-E) that recorded very different number of SO_2 exceedance events - 2 and 25, respectively (Fig. 9).

With respect to nationwide public health impacts, it was fortunate that the volcanic pollutants were predominantly transported to the north and northwest of the eruption site, likely reducing the number of SO_2 pollution episodes in the densely-populated capital to the northeast of the eruption site. The most frequent population exposure to potentially unhealthy levels of SO_2 occurred predominantly within a 20 km radius of the volcanic eruption site, in the municipalities on the Reykjanes peninsula, with up to 31 exceedance events (area G2 on Fig. 9). Individuals who spent their working hours at



some distance from their place of residence may have been exposed to different levels of volcanic pollution than can be estimated from exposure analysis based on residency. For example, station G2-A in the township of Grindavík recorded one exceedance event, but many of Grindavík's residents worked at Keflavik airport which experienced higher levels of SO₂ pollution (5 events at G2-C, Fig. 9). The reverse may have applied for those residents of Vogar (station G2-E, 25 events) who worked in the Reykjavík capital area where a lower number of exceedance events was observed (0-9 events). The estimated exposure of children was likely more accurate than for adults because most children go to schools within walking distance or minimal commuting distance from their homes. The same applies to long-term hospital inpatients.

Municipality-level population datasets are relatively easily available and therefore frequently used in population exposure analysis (Caplin et al., 2019). We show that for assessing air pollution exposure even from relatively distal sources, such as this volcanic eruption (20-55 km distance from source to impacted populated areas) there are challenges with using municipality-level population data, as there are important fine-scale variations. Furthermore, even the exceptionally dense-reference grade air quality network in this part of Iceland was unable to fully spatially resolve the pollution dispersion and frequency of above-threshold events.

3.5.2 Exposure of eruption site visitors

An interesting aspect of the eruption was that it was generally considered a very positive event by the Icelandic public (Ilyinskaya et al., 2024), and even though it took place in an uninhabited location the site became akin to a densely populated area due to the extremely high number of visitors. A considerable effort was made by the national and local authorities to minimise the risk from volcanic and general outdoor hazards. A network of three footpaths was developed, starting at designated parking areas (Fig. 10a). The footpaths were modified several times over the course of the eruption as the lava field expanded and optimal viewing areas kept changing (Barsotti et al., 2023).

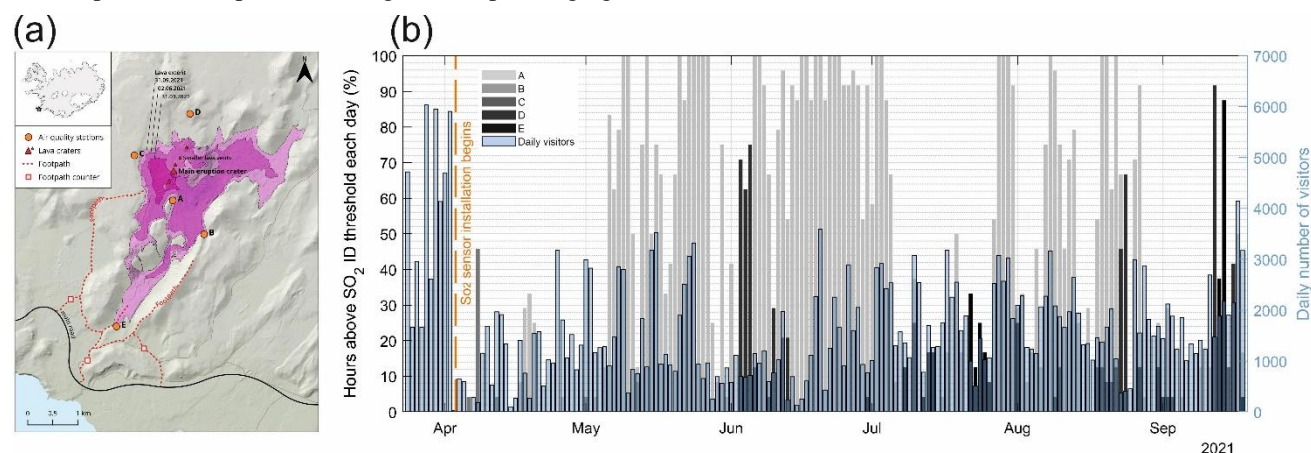


Figure 10: Eruption site visitor numbers 23 March – 19 September 2024 and potential exposure to above-threshold SO₂ concentrations estimated from eruption-site sensor data that were installed in April (stations A, B) and June (stations C, D, E). Panel (a) Topographic map of the Fagradalsfjall eruption site area showing the locations of the eruption craters, and the extent of the lava field throughout the eruption. It also shows the locations of the five G1 SO₂ air quality sensors (A-E), the footpaths which



520 were the most likely locations for visitors, and the location of the footpath visitor counters. Panel (b) shows the number of visitors per day, and the number of hours where SO₂ was above ID air quality threshold (350 µg/m³ hourly-mean) at each station. The number of hours is shown as % of day duration (n of hours/24*100). Source and copyright of basemap and cartographic elements: Icelandic Met Office & Icelandic Institute of Natural History.

We estimated the number of people who visited the eruption site by using data from automated footpath counters installed by the Icelandic Tourist Board from 24 March 2021, one on each main footpath leading to the eruption site and viewpoints (Fig. 10a). The counters were PYRO-Box with an accuracy of 95% and a sensing capacity of 4 m in both directions (Eco Counter, 525 2021). Although the vast majority of visitors used the footpath network to reach the eruption site and viewpoints, some may have walked outside the bounds of the Eco-Counter instrument range and so were not counted. There was also a number of people who landed at the eruption site on helicopter sightseeing tours who were not counted. Children who were carried, and people with permission to travel by vehicle (such as scientists and rescue teams) were also not included in the count. The visitor numbers used here are therefore a minimum estimate. The data on visitors to the site did not include details of the age 530 demographics and as such no identification of exposure of more-vulnerable age categories could be determined.

During the footpath monitoring period (24 March to 18 September 2021), the site was visited by ~300,000 people, averaging 1,600 visitors per day. The eruption-response SO₂ air quality sensors (G1) were set up along the same footpaths and we used these measurements to assess the potential exposure levels of the visitors (Fig. 10). This is based on the assumption that the concentrations measured at the stations are representative of the rest of the footpaths and other locations of the eruption site 535 visited by people, and therefore includes considerable error margins. The highest visitor numbers were in the first weeks of the eruption that coincided with Easter vacation period, with a daily average of 3,300 visitors, and a peak of 6,000 visitors on March 28. G1 stations were not set up until 3 April, therefore we have no indication of the potential exposure during the most-frequently visited period. Figure 10b shows the frequency of ID exceedance events (350 µg/m³ hourly-mean SO₂) at each of the 5 monitoring stations, and the number of daily visitors counted on the footpaths. The likelihood of exposure to 540 above-threshold SO₂ was predominantly in the vicinity of station G1-A, which recorded a cumulative total of 1600 hours above the threshold. Station G1-C had the second highest exposure with cumulative total 110 hourly-exceedances. The other three stations recorded relatively low number of exceedances, between 0 and 20 events. G1-C and G1-D were more frequently downwind of the active vents compared to the other G1 stations (wind rose in Fig. B11), and the local-scale topography played a role. In addition, based on our visual observations of this eruption, and comparable fissure eruptions, a 545 plume from a fissure eruption can occasionally collapse and spread laterally. This leads to extremely high concentrations of SO₂ even at locations upwind of the volcanic vent.

Our estimate of visitors' exposure to above-threshold events is likely a worst-case scenario because of mitigation actions. The visitors were clearly advised to remain upwind of the active craters and the lava field, and the site was staffed by rescue team members and/or rangers carrying hand-held SO₂ monitors. When SO₂ concentrations exceeded threshold levels on the 550 sensors, the visitors were urged to move into cleaner air. It is still quite likely that some visitors were exposed to unhealthy levels of SO₂ because the area was large enough that rangers with hand-held sensors were not near to all visitors and rapid changes in wind direction often brought SO₂ to areas that had clean air moments before. This is supported by anecdotal



555 reports in the Icelandic media regarding individuals seeking health care after visiting the eruption site, reportedly feeling unwell from the gas emissions. The footpath network leading to the eruption viewpoints included an elevation ascent of 200 m, so visitors were undergoing physical exertion with elevated breathing and heartrate while they were within 3 km of the eruption. High levels of physical exertion during exposure to air pollution can increase the exposure of the respiratory system which may result in more significant health impacts (Koenig et al., 1983; Qin et al., 2019).

4 Conclusions

560 The Fagradalsfjall 2021 eruption was the beginning of a prolonged eruptive period on the Reykjanes peninsula, which is ongoing at the time of writing. All investigations into the recent eruptions may prove useful for risk reduction efforts for years, and generations, to come.

565 Understanding the volcanic air pollution in a uniquely Icelandic event like the Reykjanes Fires has important implications for how we manage and prepare for other eruptions globally. The fine temporal and spatial variability in the volcanic pollution dispersion that we have discovered in this study calls for further investigation in eruptions in Iceland and other areas exposed to volcanic activity.

We show that even the exceptionally-dense reference grade air quality monitoring network in Iceland could not fully resolve the fine spatial fluctuations in volcanic air pollution episodes. We suggest that air quality networks are augmented, for example with well-calibrated lower-cost sensors, so that increased monitoring can be put in place to protect the most vulnerable individuals in the society, such as at schools and hospitals.

570



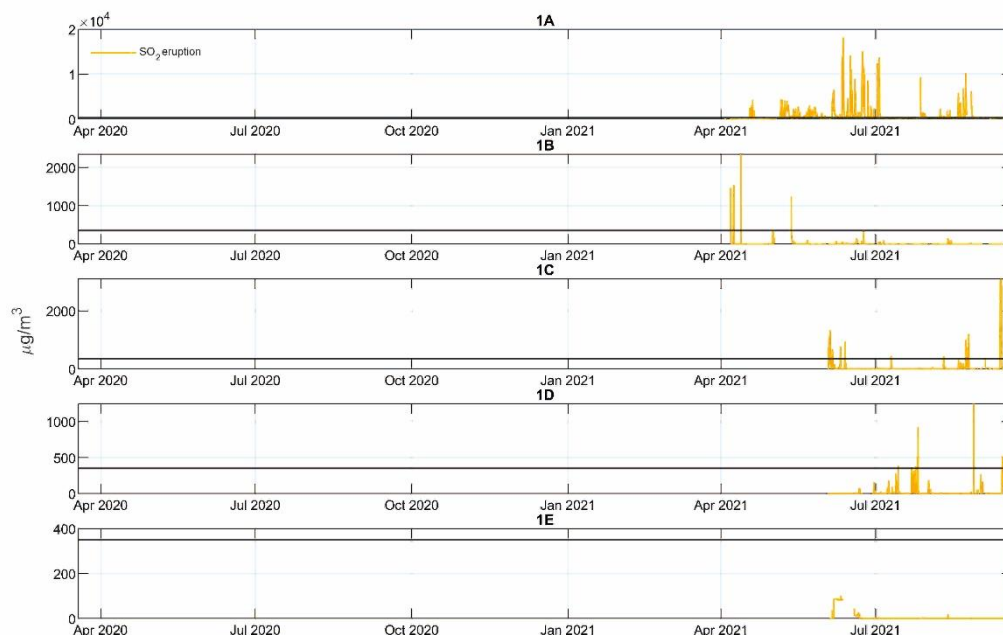
Table S1

Excel file 'Table_S1.xlsx'. Information about instrumentation, data completeness, data exclusion, etc, for each SO₂ and PM monitoring station. Summary statistics for SO₂ (hourly-means), PM₁₀, PM_{2.5} and PM₁ (daily-means) data during the background and eruption periods. SO₂ concentration data (ug/m³) reported to 2 s.f.

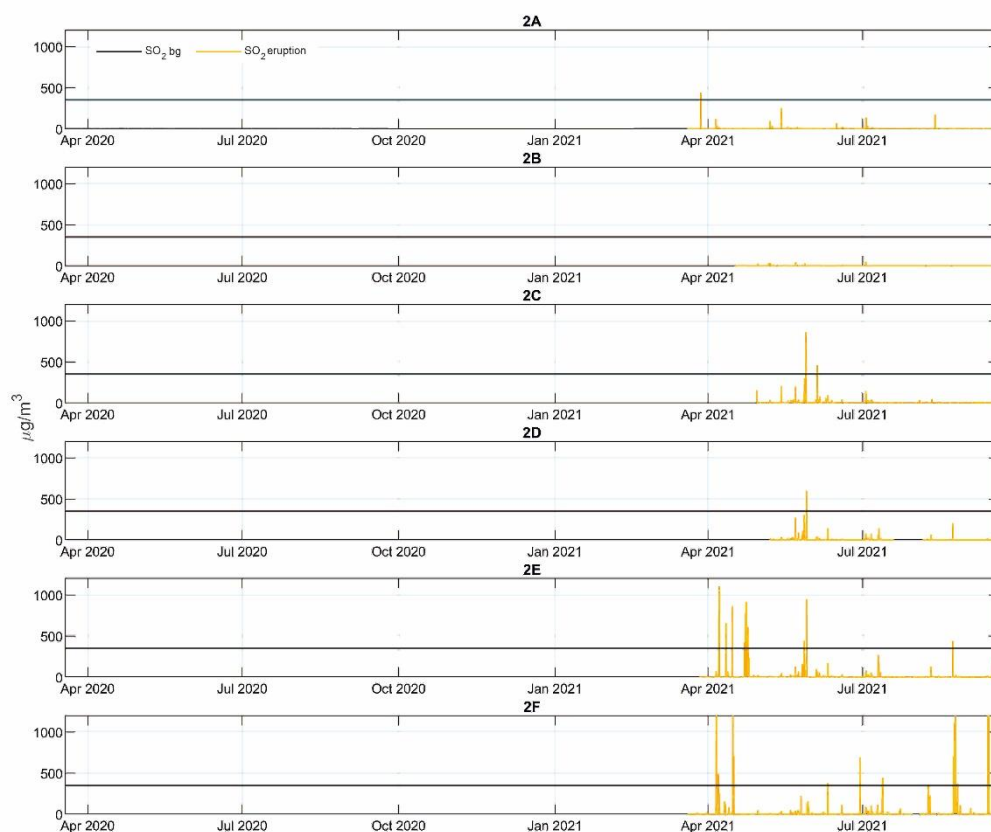
575



Appendix B.

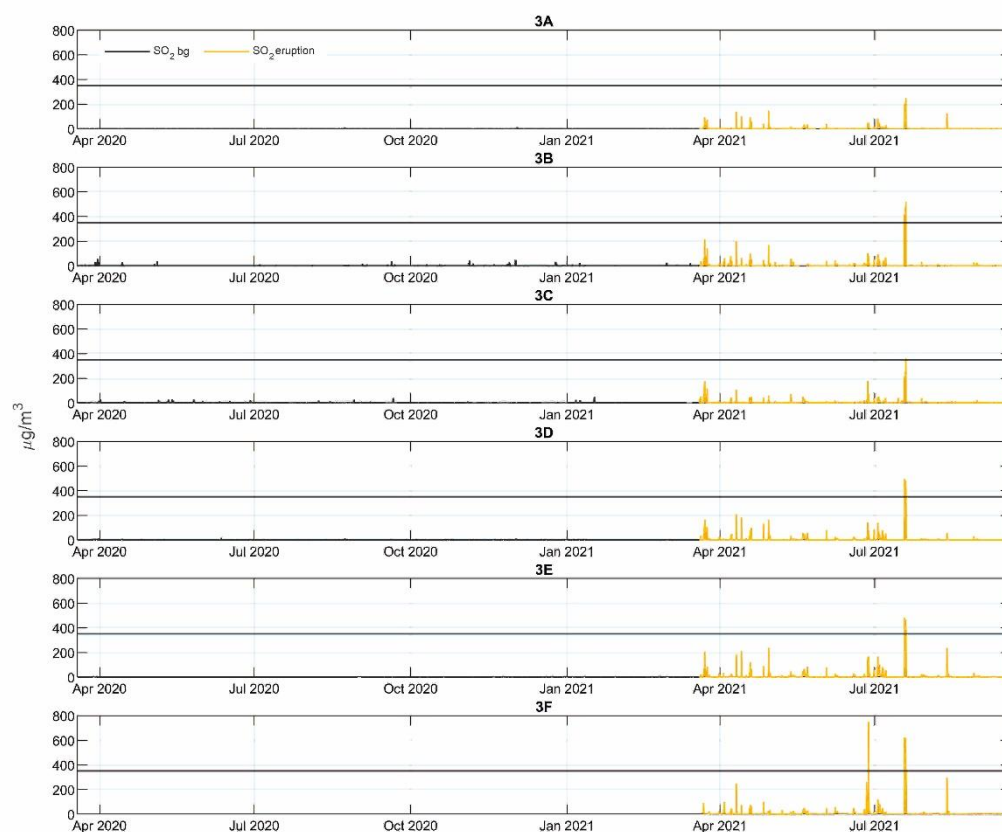


580 **Figure B1 Time series of hourly-mean concentrations SO_2 ($\mu\text{g}/\text{m}^3$), measured by the eruption site stations (G1 A-E) during the 2021 eruption. The stations were not in operation before the eruption and therefore there are no data on pre-eruptive background. The ID air quality threshold of $350 \mu\text{g}/\text{m}^3$ hourly-mean is shown on all panels with a black horizontal line. Note that the eruption-site sensors have low accuracy and were only used in this study to indicate time periods that were over the ID threshold, the absolute concentration values were not included in the analysis.**



585

Figure B2 Time series of hourly-mean concentrations SO_2 ($\mu\text{g}/\text{m}^3$), measured by Reykjanes peninsula reference-grade air quality stations (G2 A-F) during the 2021 eruption and the non-eruptive background in 2020 (bg). The ID air quality threshold of $350 \mu\text{g}/\text{m}^3$ hourly-mean is shown on all panels with a black horizontal line.



590

Figure B3 Time series of hourly-mean concentrations SO_2 ($\mu\text{g}/\text{m}^3$), measured by Reykjavík capital area reference-grade air quality stations (G3 A-F) during the 2021 eruption and the non-eruptive background in 2020 (bg). The ID air quality threshold of $350 \mu\text{g}/\text{m}^3$ hourly-mean is shown on all panels with a black horizontal line.

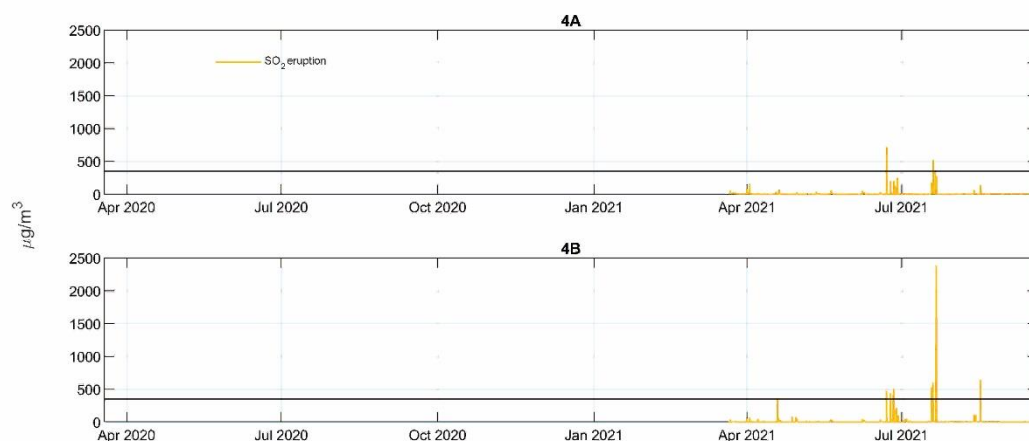


Figure B4 Time series of hourly-mean concentrations SO_2 ($\mu\text{g}/\text{m}^3$), measured in Southwest Iceland by reference-grade air quality stations (G4 A-B) during the 2021 eruption. The stations were not in operation before the eruption and therefore there are no data on pre-eruptive background. The ID air quality threshold of $350 \mu\text{g}/\text{m}^3$ hourly-mean is shown on all panels with a black horizontal line.

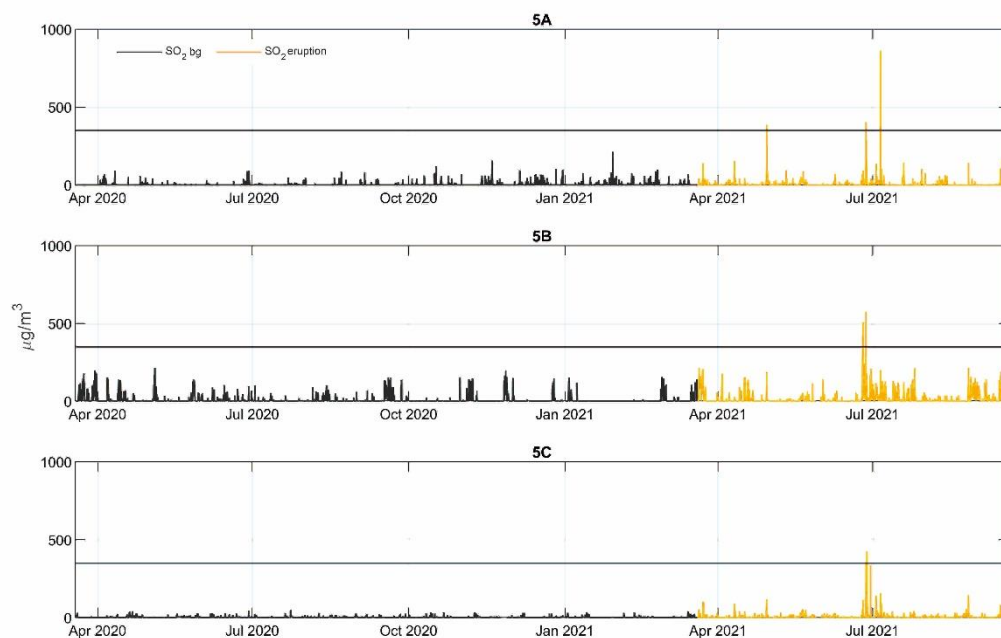


Figure B5 Time series of hourly-mean concentrations SO_2 ($\mu\text{g}/\text{m}^3$), measured in Hvalfjörður area by reference-grade air quality stations (G5 A-C) during the 2021 eruption and the non-eruptive background in 2020 (bg). The ID air quality threshold of $350 \mu\text{g}/\text{m}^3$ hourly-mean is shown on all panels with a black horizontal line.

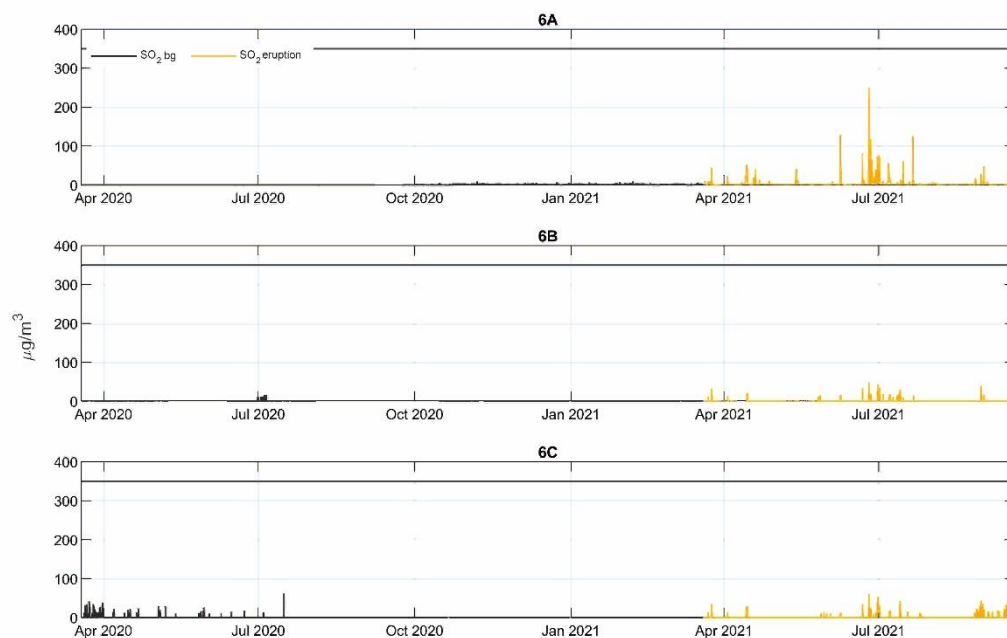


Figure B6 Time series of hourly-mean concentrations SO_2 ($\mu\text{g}/\text{m}^3$), measured in North Iceland by reference-grade air quality stations (G6 A-C) during the 2021 eruption and the non-eruptive background in 2020 (bg). The ID air quality threshold of $350 \mu\text{g}/\text{m}^3$ hourly-mean is shown on all panels with a black horizontal line.

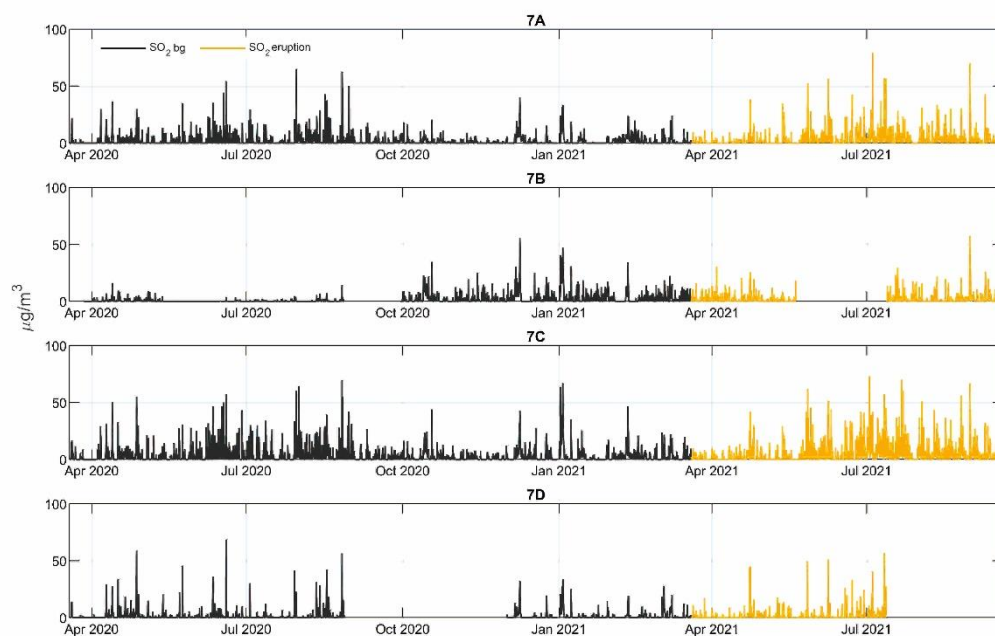


Figure B7 Time series of hourly-mean concentrations SO_2 ($\mu\text{g}/\text{m}^3$), measured in East Iceland by reference-grade air quality stations (G7 A-D) during the 2021 eruption and the non-eruptive background in 2020 (bg). The ID air quality threshold of $350 \mu\text{g}/\text{m}^3$ hourly-mean is shown on all panels with a black horizontal line.

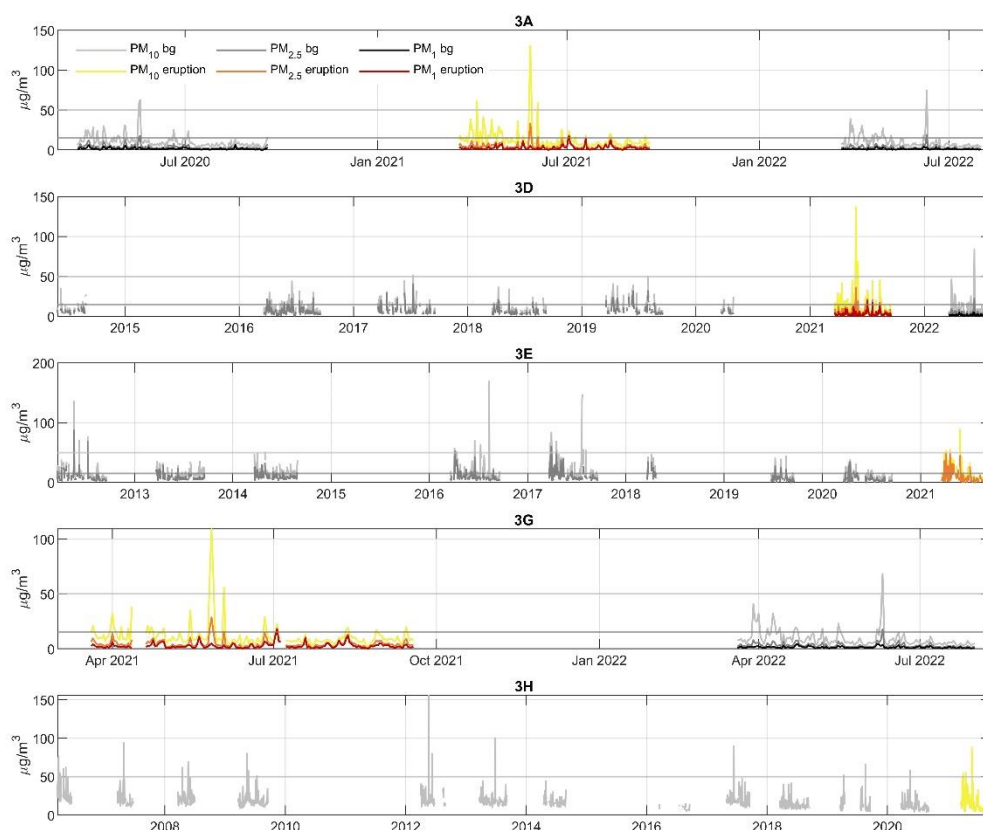


Figure B8 Time series of daily-mean concentrations of PM₁₀, PM_{2.5} and PM₁ ($\mu\text{g}/\text{m}^3$) measured in Reykjavík capital area by reference-grade air quality stations (G3 A, D, E, G, H) during the 2021 eruption and in the non-eruptive background (bg). The amount of non-eruptive background data varies between stations based on their installation date. The figures only include data for the period 19 March 20:00 – 19 September 00:00 UTC in each year, i.e. the period corresponding to the calendar dates and months of the 2021 eruption. See main text for the justification of this approach. The figures show the ID air quality thresholds for PM₁₀ and PM_{2.5} of 50 and 15 $\mu\text{g}/\text{m}^3$ daily-mean, respectively as grey horizontal lines. For PM₁, air quality thresholds have not been determined.

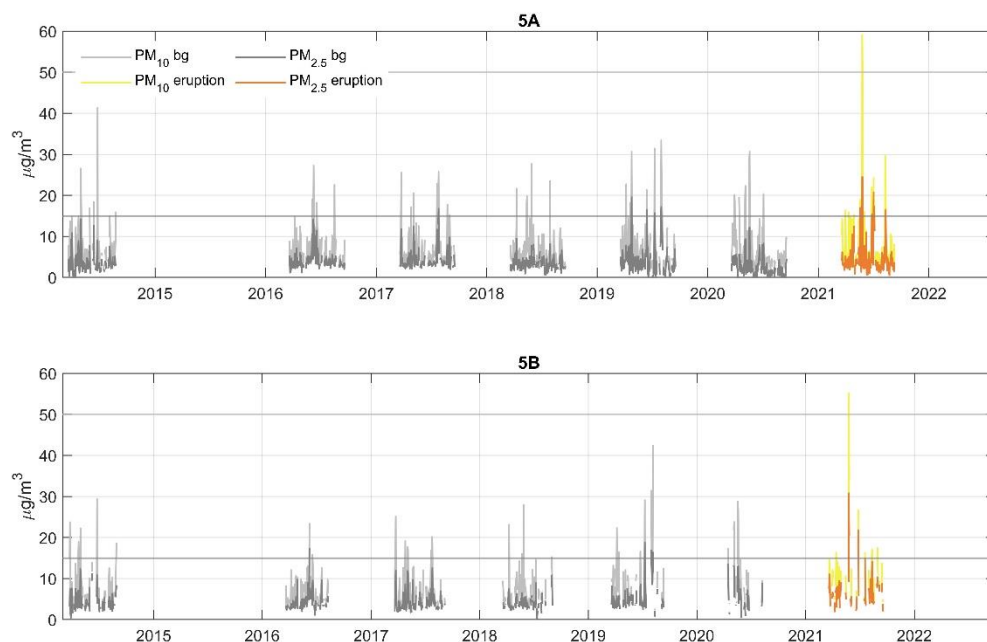


Figure B9 Time series of daily-mean concentrations of PM_{10} and $\text{PM}_{2.5}$ ($\mu\text{g}/\text{m}^3$) measured in Hvalfjörður area by reference-grade air quality stations (G5 A, B) during the 2021 eruption and in the non-eruptive background (bg). PM_1 was not measured at these stations. The amount of non-eruptive background data varies between stations based on their installation date. The figures only include data for the period 19 March 20:00 – 19 September 00:00 UTC in each year, i.e. the period corresponding to the calendar dates and months of the 2021 eruption. See main text for the justification of this approach. The figures show the ID air quality thresholds for PM_{10} and $\text{PM}_{2.5}$ of 50 and 15 $\mu\text{g}/\text{m}^3$ daily-mean, respectively as grey horizontal lines.

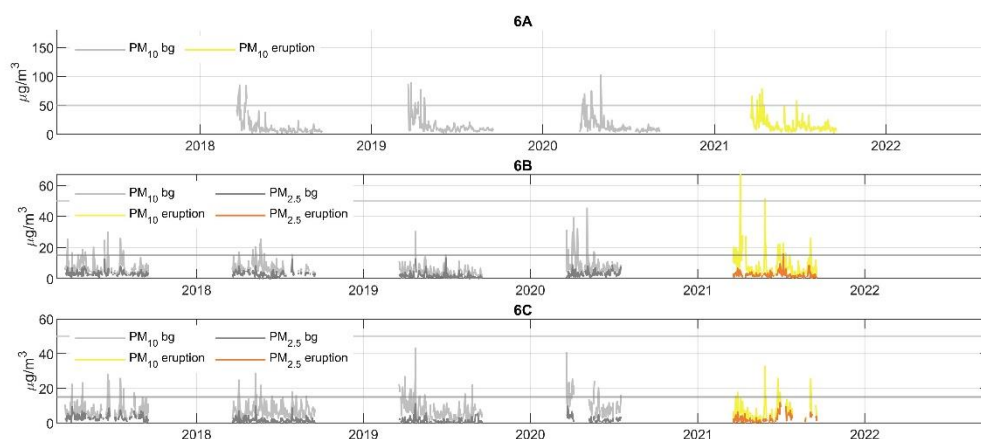
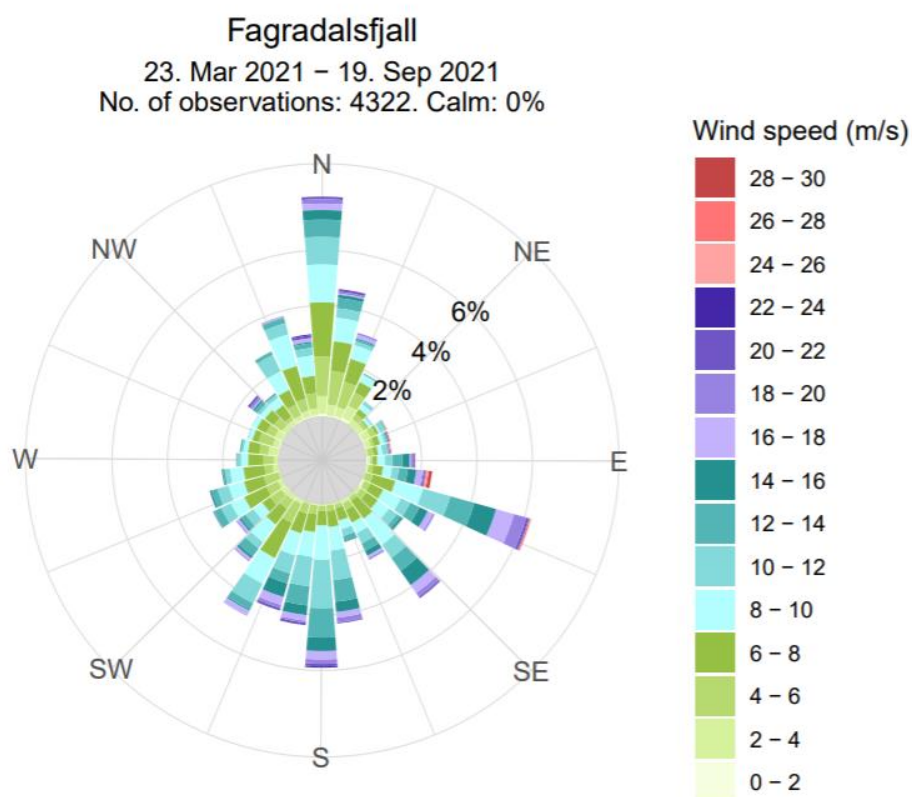


Figure B10 Time series of daily-mean concentrations of PM_{10} and $\text{PM}_{2.5}$ ($\mu\text{g}/\text{m}^3$) measured in North Iceland by reference-grade air quality stations (G6 A, B, C) during the 2021 eruption and in the non-eruptive background (bg). PM_1 was not measured at these stations. The figures only include data for the period 19 March 20:00 – 19 September 00:00 UTC in each year, i.e. the period corresponding to the calendar dates and months of the 2021 eruption. See main text for the justification of this approach. The figures show the ID air quality thresholds for PM_{10} and $\text{PM}_{2.5}$ of 50 and 15 $\mu\text{g}/\text{m}^3$ daily-mean, respectively as grey horizontal lines.



640

Figure B11 Windrose shows wind direction and wind speed measured by Icelandic Meteorological Office weather station at the Fagradalsfjall eruption site 23 March – 19 September 2021.



645 **Data availability**

Full dataset of SO₂, PM₁₀, PM_{2.5} and PM₁ concentrations is openly available for download from the Environment Agency of Iceland <https://loftgaedi.is/en>

Author contributions

650 RCWW performed the original data analysis and drafted the original manuscript and figures. SB, MAP, TR and AS contributed to data interpretation and manuscript drafting. EI finalised the data analysis, the manuscript and produced Figs. 2-7, 9 and Appendix B B1-B10. RHTh produced Figs. 1, 8, and 9. TH, GMG and MAP designed, built and maintained IMO's measurement and data systems. TJ contributed access to and information on the reference-grade AQ network and quality-controlled data. DF and RHTh led on the ArcGIS ArcMap analysis methodology. GGS supplied the data from footpath counters. All coauthors contributed to draft review and editing.

655 **Competing interests**

The authors declare that they have no conflict of interest.

Acknowledgements

The authors would like to thank Kristín Björg Ólafsdóttir from the Icelandic Meteorological Office for analysis of wind data and creation of the wind rose in Appendix B Fig. B11.

660 **Financial support**

RCWW is funded by the Leeds-York Natural Environment Research Council (NERC) Doctoral Training Partnership (DTP) NE/L002574/1, in CASE partnership with the Icelandic Meteorological Office. TJR is funded by the ANR Projet de Recherche Collaborative VOLC-HAL-CLIM (Volcanic Halogens: from Deep Earth to Atmospheric Impacts) ANR-18-CE01-0018, and Labex Orléans Labex VOLTAIRE (VOLatils-Terre Atmosphère Interactions–Ressources et
665 Environnement, ANR-10-LABX-100-0). EI acknowledges NERC Centre for Observation and Modelling of Earthquakes, Volcanoes and Tectonics (COMET+), a partnership between UK Universities and the British Geological Survey; NERC Highlight Topic V-PLUS NE/S00436X/1 and NERC Urgency Grant NE/Z000262/1 “Chemistry of emissions at lava-urban interfaces”.



References

- 670 Barsotti, S., Parks, M. M., Pfeffer, M. A., Óladóttir, B. A., Barnie, T., Titos, M. M., Jónsdóttir, K., Pedersen, G. B. M., Hjartardóttir, Á. R., Stefansdóttir, G., Johannsson, T., Arason, Þ., Gudmundsson, M. T., Oddsson, B., Þrastarson, R. H., Ófeigsson, B. G., Vogfjörð, K., Geirsson, H., Hjörvar, T., von Löwis, S., Petersen, G. N., and Sigurðsson, E. M.: The eruption in Fagradalsfjall (2021, Iceland): how the operational monitoring and the volcanic hazard assessment contributed to its safe access, *Nat. Hazards*, <https://doi.org/10.1007/s11069-022-05798-7>, 2023.
- 675 Butwin, M. K., von Löwis, S., Pfeffer, M. A., and Thorsteinsson, T.: The effects of volcanic eruptions on the frequency of particulate matter suspension events in Iceland, *J. Aerosol Sci.*, 128, 99–113, 2019.
- Caplin, A., Ghandehari, M., Lim, C., Glimcher, P., and Thurston, G.: Advancing environmental exposure assessment science to benefit society, *Nat. Commun.*, 10, 1236, <https://doi.org/10.1038/s41467-019-09155-4>, 2019.
- 680 Carlsen, H. K. and Thorsteinsson, T.: Associations between PM₁₀ from Traffic, Resuspension, Sand Storms and Volcanic Sources and Asthma Drugs Dispensing, *In Review*, <https://doi.org/10.21203/rs.3.rs-1017409/v1>, 2021.
- Carlsen, H. K., Ilyinskaya, E., Baxter, P. J., Schmidt, A., Thorsteinsson, T., Pfeffer, M. A., Barsotti, S., Dominici, F., Finnbjörnsdóttir, R. G., Jóhannsson, T., Aspelund, T., Gislason, T., Valdimarsdóttir, U., Briem, H., and Gudnason, T.: Increased respiratory morbidity associated with exposure to a mature volcanic plume from a large Icelandic fissure eruption, *Nat. Commun.*, 12, 2161, <https://doi.org/10.1038/s41467-021-22432-5>, 2021a.
- 685 Carlsen, H. K., Valdimarsdóttir, U., Briem, H., Dominici, F., Finnbjörnsdóttir, R. G., Jóhannsson, T., Aspelund, T., Gislason, T., and Gudnason, T.: Severe volcanic SO_2 exposure and respiratory morbidity in the Icelandic population—a register study, *Environ. Health*, 20, 1–12, 2021b.
- Chen, G., Li, S., Zhang, Y., Zhang, W., Li, D., Wei, X., He, Y., Bell, M. L., Williams, G., Marks, G. B., and others: Effects of ambient PM_{2.5} air pollution on daily emergency hospital visits in China: an epidemiological study, *Lancet Planet. Health*, 1, e221–e229, 2017.
- 690 Crawford, B., Hagan, D. H., Grossman, I., Cole, E., Holland, L., Heald, C. L., and Kroll, J. H.: Mapping pollution exposure and chemistry during an extreme air quality event (the 2018 Kīlauea eruption) using a low-cost sensor network, *Proc. Natl. Acad. Sci.*, 118, 2021.
- Crilley, L. R., Shaw, M., Pound, R., Kramer, L. J., Price, R., Young, S., Lewis, A. C., and Pope, F. D.: Evaluation of a low-cost optical particle counter (Alphasense OPC-N2) for ambient air monitoring, *Atmospheric Meas. Tech.*, 709–720, 2018.
- 695 Eco Counter: PYRO-Box, <https://www.eco-counter.com/products/pyro-range/pyro-box>, 2021.
- Freire, S., Florczyk, A. J., Pesaresi, M., and Sliuzas, R.: An Improved Global Analysis of Population Distribution in Proximity to Active Volcanoes, 1975–2015, *ISPRS Int. J. Geo-Inf.*, 8, 341, <https://doi.org/10.3390/ijgi8080341>, 2019.
- 700 Gíslason, S. R., Stefánsdóttir, G., Pfeffer, M. A., Barsotti, S., Jóhannsson, Th., Galeczka, I., Bali, E., Sigmarsson, O., Stefánsson, A., Keller, N. S., Sigurdsson, á., Bergsson, B., Galle, B., Jacobo, V. C., Arellano, S., Aiuppa, A., Jónasdóttir, E. B., Eiríksdóttir, E. S., Jakobsson, S., Guðfinnsson, G. H., Halldórsson, S. A., Gunnarsson, H., Haddadi, B., Jónsdóttir, I., Thordarson, Th., Riishuus, M., Högnadóttir, Th., Dürig, T., Pedersen, G. B. M., Höskuldsson, á., and Gudmundsson, M. T.: Environmental pressure from the 2014–15 eruption of Bárðarbunga volcano, Iceland, *Geochem. Perspect. Lett.*, 84–93, <https://doi.org/10.7185/geochemlet.1509>, 2015.



- 705 Green, J. R., Fiddler, M. N., Holloway, J. S., Fibiger, D. L., McDuffie, E. E., Campuzano-Jost, P., Schroder, J. C., Jimenez, J. L., Weinheimer, A. J., Aquino, J., and others: Rates of wintertime atmospheric SO_2 oxidation based on aircraft observations during clear-sky conditions over the eastern United States, *J. Geophys. Res. Atmospheres*, 124, 6630–6649, 2019.
- 710 Icelandic Directive: Reglugerð um brennisteinsdíoxíð, köfnunarefnisdíoxíð og köfnunarefnisoxíð, bensen, kolsýring, svifryk og blý í andrúmsloftinu, B-Deild, Nr.920, 2016.
- Ilyinskaya, E., Schmidt, A., Mather, T. A., Pope, F. D., Witham, C., Baxter, P., Jóhannsson, T., Pfeffer, M., Barsotti, S., Singh, A., Sanderson, P., Bergsson, B., McCormick Kilbride, B., Donovan, A., Peters, N., Oppenheimer, C., and Edmonds, M.: Understanding the environmental impacts of large fissure eruptions: Aerosol and gas emissions from the 2014–2015 Holuhraun eruption (Iceland), *Earth Planet. Sci. Lett.*, 472, 309–322, <https://doi.org/10.1016/j.epsl.2017.05.025>, 2017.
- 715 Ilyinskaya, E., Mason, E., Wieser, P. E., Holland, L., Liu, E. J., Mather, T. A., Edmonds, M., Whitty, R. C. W., Elias, T., Nadeau, P. A., Schneider, D., McQuaid, J. B., Allen, S. E., Harvey, J., Oppenheimer, C., Kern, C., and Damby, D.: Rapid metal pollutant deposition from the volcanic plume of Kīlauea, Hawai‘i, *Commun. Earth Environ.*, 2, 1–15, <https://doi.org/10.1038/s43247-021-00146-2>, 2021.
- 720 Ilyinskaya, E., Snæbjarnarson, V., Carlsen, H. K., and Oddsson, B.: Brief communication: Small-scale geohazards cause significant and highly variable impacts on emotions, *Nat. Hazards Earth Syst. Sci.*, 24, 3115–3128, <https://doi.org/10.5194/nhess-24-3115-2024>, 2024.
- Koenig, J. Q., Pierson, W. E., and Horike, M.: The effects of inhaled sulfuric acid on pulmonary function in adolescent asthmatics, *Am. Rev. Respir. Dis.*, 128, 221–225, <https://doi.org/10.1164/arrd.1983.128.2.221>, 1983.
- 725 Martin, R. S., Ilyinskaya, E., Sawyer, G. M., Tsanev, V. I., and Oppenheimer, C.: A re-assessment of aerosol size distributions from Masaya volcano (Nicaragua), *Atmos. Environ.*, 45, 547–560, <https://doi.org/10.1016/j.atmosenv.2010.10.049>, 2011.
- 730 Mason, E., Wieser, P. E., Liu, E. J., Edmonds, M., Ilyinskaya, E., Whitty, R. C. W., Mather, T. A., Elias, T., Nadeau, P. A., Wilkes, T. C., McGonigle, A. J. S., Perring, T. D., Mims, F. M., Kern, C., Schneider, D. J., and Oppenheimer, C.: Volatile metal emissions from volcanic degassing and lava–seawater interactions at Kīlauea Volcano, Hawai‘i, *Commun. Earth Environ.*, 2, 1–16, <https://doi.org/10.1038/s43247-021-00145-3>, 2021.
- Pattantyus, A. K., Businger, S., and Howell, S. G.: Review of sulfur dioxide to sulfate aerosol chemistry at Kīlauea Volcano, Hawai‘i, *Atmos. Environ.*, 185, 262–271, <https://doi.org/10.1016/j.atmosenv.2018.04.055>, 2018.
- 735 Pfeffer, M. A., Arellano, S., Barsotti, S., Petersen, G. N., Barnie, T., Ilyinskaya, E., Hjörvar, T., Bali, E., Pedersen, G. B. M., Guðmundsson, G. B., Vogfjörð, K., Ranta, E. J., Óladóttir, B. A., Edwards, B. A., Moussallam, Y., Stefánsson, A., Scott, S. W., Smekens, J.-F., Varnam, M., and Titos, M.: SO_2 emission rates and incorporation into the air pollution dispersion forecast during the 2021 eruption of Fagradalsfjall, Iceland, *J. Volcanol. Geotherm. Res.*, 449, 108064, <https://doi.org/10.1016/j.jvolgeores.2024.108064>, 2024.
- Qin, F., Yang, Y., Wang, S., Dong, Y., Xu, M., Wang, Z., and Zhao, J.: Exercise and air pollutants exposure: A systematic review and meta-analysis, *Life Sci.*, 218, 153–164, <https://doi.org/10.1016/j.lfs.2018.12.036>, 2019.
- 740 Schmidt, A., Leadbetter, S., Theys, N., Carboni, E., Witham, C. S., Stevenson, J. A., Birch, C. E., Thordarson, T., Turnock, S., Barsotti, S., Delaney, L., Feng, W., Grainger, R. G., Hort, M. C., Höskuldsson, Á., Ialongo, I., Ilyinskaya, E., Jóhannsson, T., Kenny, P., Mather, T. A., Richards, N. A. D., and Shepherd, J.: Satellite detection, long-range transport and air quality



- impacts of volcanic sulfur dioxide from the 2014–15 flood lava eruption at Bárðarbunga (Iceland), *J. Geophys. Res. Atmospheres*, 2015JD023638, <https://doi.org/10.1002/2015JD023638>, 2015.
- 745 Siebert, L., Cottrell, E., Venzke, E., and Andrews, B.: Chapter 12 - Earth's Volcanoes and Their Eruptions: An Overview, in: *The Encyclopedia of Volcanoes (Second Edition)*, edited by: Sigurdsson, H., Academic Press, Amsterdam, 239–255, <https://doi.org/10.1016/B978-0-12-385938-9.00012-2>, 2015.
- Stewart, C., Damby, D. E., Horwell, C. J., Elias, T., Ilyinskaya, E., Tomašek, I., Longo, B. M., Schmidt, A., Carlsen, H. K., Mason, E., Baxter, P. J., Cronin, S., and Witham, C.: Volcanic air pollution and human health: recent advances and future
750 directions, *Bull. Volcanol.*, 84, 11, <https://doi.org/10.1007/s00445-021-01513-9>, 2021.
- Wang, Y., Guo, J., Wang, T., Ding, A., Gao, J., Zhou, Y., Collett, J. L., and Wang, W.: Influence of regional pollution and sandstorms on the chemical composition of cloud/fog at the summit of Mt. Taishan in northern China, *Atmospheric Res.*, 99, 434–442, <https://doi.org/10.1016/j.atmosres.2010.11.010>, 2011.
- Whitty, R., Pfeffer, M., Ilyinskaya, E., Roberts, T., Schmidt, A., Barsotti, S., Strauch, W., Crilley, L., Pope, F., Bellanger, H., Mendoza, E., Mather, T., Liu, E., Peters, N., Taylor, I., Francis, H., Leiva, X. H., Lynch, D., Nobert, S., and Baxter, P.: Effectiveness of low-cost air quality monitors for identifying volcanic SO₂ and PM downwind from Masaya volcano, Nicaragua, *Volcanica*, 5, 33–59, <https://doi.org/10.30909/vol.05.01.3359>, 2022.
- 755 Whitty, R. C. W., Ilyinskaya, E., Mason, E., Wieser, P. E., Liu, E. J., Schmidt, A., Roberts, T., Pfeffer, M. A., Brooks, B., Mather, T. A., Edmonds, M., Elias, T., Schneider, D. J., Oppenheimer, C., Dybwad, A., Nadeau, P. A., and Kern, C.: Spatial and Temporal Variations in SO₂ and PM_{2.5} Levels Around Kīlauea Volcano, Hawai'i During 2007–2018, *Front. Earth Sci.*, 8, <https://doi.org/10.3389/feart.2020.00036>, 2020.
- 760 World Health Organization: WHO global air quality guidelines: particulate matter (PM_{2.5} and PM₁₀), ozone, nitrogen dioxide, sulfur dioxide and carbon monoxide, World Health Organization, xxi, 267 pp., 2021.
- Yang, M., Chu, C., Bloom, M. S., Li, S., Chen, G., Heinrich, J., Markevych, I., Knibbs, L. D., Bowatte, G., Dharmage, S. C., and others: Is smaller worse? New insights about associations of PM_{2.5} and respiratory health in children and
765 adolescents, *Environ. Int.*, 120, 516–524, 2018.